NeuroImage 271 (2023) 120027

Contents lists available at ScienceDirect

NeuroImage

journal homepage: www.elsevier.com/locate/neuroimage

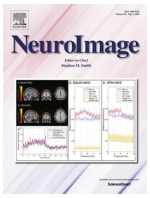

Cortico-cortical paired associative stimulation (ccPAS) over premotor-motor areas affects local circuitries in the human motor cortex via Hebbian plasticity

Sonia Turrini [a,b,*], Francesca Fiori [a,c,1], Emilio Chiappini [a,d,1], Boris Lucero [e], Emiliano Santarnecchi [b], Alessio Avenanti [a,e,*]

[a] Centro studi e Ricerche in Neuroscienze Cognitive, Dipartimento di Psicologia "Renzo Canestrari", Alma Mater Studiorum Università di Bologna, Cesena Campus, Cesena 47521, Italy
[b] Precision Neuroscience & Neuromodulation Program, Gordon Center for Medical Imaging, Massachusetts General Hospital & Harvard Medical School, Boston, MA 02114, United States
[c] NeXT: Neurophysiology and Neuro-Engineering of Human-Technology Interaction Research Unit, Campus Bio-Medico University, Rome 00128, Italy
[d] Institut für Klinische und Gesundheitspsychologie, Universität Wien, Vienna 1010, Austria
[e] Centro de Investigación en Neuropsicología y Neurociencias Cognitivas (CINPSI Neurocog), Universidad Católica Del Maule, Talca 346000, Chile

ARTICLE INFO

Keywords:
Hebbian plasticity
Cortico-cortical connectivity
Long-term potentiation
Motor cortex
Transcranial magnetic stimulation
Intracortical inhibition

ABSTRACT

Transcranial magnetic stimulation (TMS) studies have shown that cortico-cortical paired associative stimulation (ccPAS) can strengthen connectivity between the ventral premotor cortex (PMv) and the primary motor cortex (M1) by modulating convergent input over M1 via Hebbian spike-timing-dependent plasticity (STDP). However, whether ccPAS locally affects M1 activity remains unclear. We tested 60 right-handed young healthy humans in two studies, using a combination of dual coil TMS and ccPAS over the left PMv and M1 to probe and manipulate PMv-to-M1 connectivity, and single- and paired-pulse TMS to assess neural activity within M1. We provide convergent evidence that ccPAS, relying on repeated activations of excitatory PMv-to-M1 connections, acts locally over M1. During ccPAS, motor-evoked potentials (MEPs) induced by paired PMv-M1 stimulation gradually increased. Following ccPAS, the threshold for inducing MEPs of different amplitudes decreased, and the input-output curve (IO) slope increased, highlighting increased M1 corticospinal excitability. Moreover, ccPAS reduced the magnitude of short-interval intracortical inhibition (SICI), reflecting suppression of GABA-ergic interneuronal mechanisms within M1, without affecting intracortical facilitation (ICF). These changes were specific to ccPAS Hebbian strengthening of PMv-to-M1 connectivity, as no modulations were observed when reversing the order of the PMv-M1 stimulation during a control ccPAS protocol. These findings expand prior ccPAS research that focused on the malleability of cortico-cortical connectivity at the network-level, and highlight local changes in the area of convergent activation (i.e., M1) during plasticity induction. These findings provide new mechanistic insights into the physiological basis of ccPAS that are relevant for protocol optimization.

1. Introduction

Motor network functioning is based on neural interactions between different premotor and motor areas. The ventral premotor cortex (PMv) and the primary motor cortex (M1) are two key cortical motor areas primarily involved in fine motor control. PMv is a component of the dorsolateral motor stream that transforms sensory stimuli, processed in parietal regions, into specific motor commands (Fogassi et al., 2001; Chen and Rothwell, 2012; Rizzolatti et al., 2014) mainly implemented via M1. Moreover, the PMv-M1 circuit is consistently involved in a number of cognitive processes including motor imagery (Jeannerod, 2001; Fourkas et al., 2008; Bencivegna et al., 2021), action perception (Avenanti et al., 2013a, 2013b; Rizzolatti et al., 2014), and language production and comprehension (Carota et al., 2017; Vitale et al., 2021, 2022). Remarkably, the functional coupling between these two nodes is highly flexible, shifting as a function of experiences ranging from motor training (Albert et al., 2009; Dayan et al., 2011; Taubert et al., 2011; Hamzei et al., 2012; Philip et al., 2016) to brain

* Corresponding authors at: Centro studi e ricerche in Neuroscienze Cognitive, Dipartimento di Psicologia "Renzo Canestrari", Alma Mater Studiorum Università di Bologna, Cesena Campus, Via Rasi Spinelli 176, Cesena 47521, Italy.
E-mail addresses: sonia.turrini3@unibo.it (S. Turrini), alessio.avenanti@unibo.it (A. Avenanti).
[1] Equal contribution

https://doi.org/10.1016/j.neuroimage.2023.120027.
Received 7 September 2022; Received in revised form 9 March 2023; Accepted 13 March 2023
Available online 15 March 2023.
1053-8119/© 2023 Published by Elsevier Inc. This is an open access article under the CC BY-NC-ND license (http://creativecommons.org/licenses/by-nc-nd/4.0/)

injuries (Nelles et al., 2001; Sun et al., 2007; Wiestler and Diedrichsen, 2013; Horn et al., 2016).

Recent advances in non-invasive brain stimulation allow not only for the modulation of activity within these individual regions, but also for the manipulation of connectivity between them via Hebbian plasticity. Cortico-cortical paired associative stimulation (ccPAS) is a dual coil transcranial magnetic stimulation (dcTMS) technique aimed at modulating the synaptic efficacy of cortico-cortical connections (Buch et al., 2011; Koch et al., 2013; Johnen et al., 2015; Romei et al., 2016a; Chiappini et al., 2018, 2020, 2022; Fiori et al., 2018; Santarecchi et al. 2018; Zibman et al., 2019; Momi et al., 2020; Di Luzio et al., 2022). The ccPAS protocol stems from the classical paired associative stimulation (PAS) protocol that employs repetitive peripheral nerve stimulation and TMS over M1 (Stefan et al., 2000; Suppa et al., 2017) to induce spike timing-dependent plasticity (STDP) – a form of plasticity based on the Hebbian rule (Hebb, 1949; Jackson et al., 2006; Caporale and Dan, 2008; Markram et al., 2011). In the ccPAS protocol, two focal coils are used to target two physiologically connected cortical areas to induce STDP between them (Caporale and Dan, 2008; Rizzo et al., 2009; Romei et al., 2016b). According to the Hebbian principle, synapses are potentiated when presynaptic neurons fire immediately before postsynaptic neurons in a coherent and repeated manner (Hebb, 1949; Jackson et al., 2006; Caporale and Dan, 2008; Markram et al., 2011). This pre- and post-synaptic pairing is modeled in the ccPAS protocol by targeting two areas with a specific pattern where the "pre-synaptic area" is repeatedly stimulated immediately before stimulation of the "post-synaptic area", with an inter-stimulus interval (ISI) between the two pulses tailored to the temporal properties of the pathway connecting the two areas. It is held that the repeated dcTMS pairing in the ccPAS protocol can increase the synaptic efficacy of the connections between the two target areas, showing long-term potentiation-like (LTP-like) effects (Buch et al., 2011; Koch et al., 2013; Romei et al., 2016b; Santarnecchi et al., 2018).

The ccPAS protocol has been successfully applied to the PMv-to-M1 pathway (Buch et al., 2011; Johnen et al., 2015; Fiori et al., 2018; Chiappini et al., 2020; Sel et al., 2021; Turrini et al., 2022, 2023), relying on extensive knowledge of PMv-M1 interactions (Ghosh and Porter, 1988; Tokuno and Nambu, 2000; Cerri et al., 2003; Shimazu et al., 2004). In humans, these interactions have been explored using dcTMS to assess cortico-cortical effective connectivity; a conditioning TMS pulse over PMv affects motor-evoked potentials (MEPs) induced by a second TMS pulse over M1 at short ISIs between PMv and M1 stimulation (i.e., 6–8 ms; Davare et al., 2008, 2009; Bäumer et al., 2009), but also at longer ISIs (e.g., 40 ms; Fiori et al., 2016, 2017) – highlighting both short- and long-latency PMv-to-M1 interactions. Building on this dcTMS evidence, other work found that ccPAS over the PMv-to-M1 circuit ($ccPAS_{PMv\rightarrow M1}$) potentiated the physiological conditioning effect of PMv stimulation on M1 corticospinal excitability, both when ccPAS targeted short- (Buch et al., 2011) and longer-latency PMv-to-M1 interactions (Chiappini et al., 2020). These studies provide evidence that ccPAS potentiates PMv-to-M1 effective connectivity via increased efficacy of PMv synaptic input to M1. These pathway-specific changes in connectivity (Buch et al., 2011; Chiappini et al., 2020) are corroborated by magnetic resonance imaging (MRI) evidence of increased functional coupling (Johnen et al., 2015). Moreover, $ccPAS_{PMv\rightarrow M1}$ aftereffects appear to be functionally specific, as demonstrated by task-dependent electroencephalography (EEG) (Sel et al., 2021) and behavioral results (Fiori et al., 2018).

All this prior work has focused on changes in cortico-cortical connectivity, without clarifying whether $ccPAS_{PMv\rightarrow M1}$ is also able to locally modulate M1 (i.e., the area of convergent activation during ccPAS protocol stimulation). Interestingly, previous ccPAS studies have used different stimulation parameters, possibly tapping into different inhibitory vs. excitatory cortico-cortical interactions. In a first study, Buch et al. (2011) assessed the conditioning effect of PMv stimulation on MEPs induced by M1 stimulation – i.e., a dcTMS measure of PMv-to-M1 effective connectivity. Suprathreshold PMv conditioning was found to reduce MEPs, and that inhibitory effect was enhanced after $ccPAS_{PMv\rightarrow M1}$, reflecting LTP of glutamatergic PMv projections on inhibitory interneurons in M1. In contrast, ccPAS did not affect M1 corticospinal excitability as measured by single-pulse TMS (spTMS) over M1 administered at a fixed intensity (see also Chiappini et al., 2020).

Three recent studies conducted in our laboratory used subthreshold PMv stimulation instead during $ccPAS_{PMv\rightarrow M1}$. Assessing MEPs "online" during protocol administration (i.e., MEPs evoked by the repeated dcTMS paired stimulation of PMv and M1), we reported a gradual increase in MEP amplitude throughout the protocol (Fiori et al., 2018; Turrini et al., 2022, 2023). This suggested a possible progressive enhancement of excitatory (rather than inhibitory) PMv-to-M1 interactions, due to the gradually increasing efficacy of excitatory synaptic input to M1 neurons. However, our prior studies did not clarify whether the adopted $ccPAS_{PMv\rightarrow M1}$ protocol (i.e., with subthreshold PMv stimulation) rests on excitatory PMv-to-M1 interactions, nor whether this protocol induces local changes in M1 activity.

A few prior studies have investigated local M1 effects when ccPAS was administered to modulate synaptic inputs from the contralateral M1 (Rizzo et al., 2009, 2011; Koganemaru et al., 2009), PMv (Lazari et al., 2022) and the cerebellum (Lu et al., 2012), or the ipsilateral parietal cortex (Koch et al., 2013; Veniero et al., 2013). These studies provided mixed results regarding ccPAS effects on M1 excitability, which may reflect network- and protocol-specific features. However, none of the previous studies systematically investigated local changes in M1 excitability following $ccPAS_{PMv\rightarrow M1}$. This issue is particularly relevant as a $ccPAS_{PMv\rightarrow M1}$ protocol with subthreshold stimulation of the ipsilateral PMv was shown to enhance hand dexterity (Fiori et al., 2018; Turrini et al., 2023). Elucidating the physiological underpinnings of $ccPAS_{PMv\rightarrow M1}$ is therefore critical in view of its potential clinical applications in motor rehabilitation.

To address this question, here, we performed two studies. In an initial pilot study, building on our previous work (Fiori et al., 2018; Turrini et al., 2022, 2023), we used dcTMS to test whether subthreshold conditioning of the left PMv would exert a facilitatory conditioning effect over the ipsilateral M1. We tested short ISIs (6, 8, 10 ms), indexing early excitatory PMv-to-M1 interactions. Results confirmed that dcTMS PMv conditioning with an 8-m ISI induced a consistent MEP facilitation, relative to MEPs induced by spTMS. Building on this pilot study, in the main experiment we administered $ccPAS_{PMv\rightarrow M1}$ with subthreshold PMv stimulation and an 8-ISI (as in Fiori et al., 2018 and Turrini et al., 2022, 2023). We assessed the online effect of $ccPAS_{PMv\rightarrow M1}$ by recording MEPs induced by dcTMS during protocol administration. Moreover, we assessed ccPAS aftereffects by recording different measures of M1 corticospinal excitability following spTMS of the left M1, namely the resting motor threshold (rMT), the TMS intensity required to elicit a MEP of 1 mV amplitude (SI_{1mV}), and the input-output (IO) curve. Additionally, we used paired-pulse TMS (ppTMS) over the left M1 to assess short interval intracortical inhibition (SICI) and intracortical facilitation (ICF) as measures of intracortical M1 excitability. As a control, in the $ccPAS_{M1\rightarrow PMv}$ group the order of the dcTMS pulses was reversed, i.e., M1 always preceded PMv stimulation, to ensure that any potential effects of $ccPAS_{PMv\rightarrow M1}$ were due to specific directional changes in effective connectivity and not to generic stimulation of PMv and M1.

The rMT provides a well-established global measure of M1 corticospinal excitability (Chen, 2000; Rossini et al., 2015). The SI_{1mV} also provides a global measure of motor excitability, which is partially distinct from rMT as it uses higher intensities which allow one to evaluate the contribution of larger neuronal populations (e.g., less excitable neurons and neurons spatially further from the targeted region). The IO curve is the sigmoidal relation between MEP amplitude and incremented TMS intensities (Ridding and Rothwell, 1997; Chen, 2000), covering and extending the intensities used for assessing rMT and SI_{1mV}; fitting the curve provides key parameters, such as its slope, inflection point and the upper asymptote, that accurately characterize this rela-

tion (Devanne et al., 1997; Houdayer et al., 2008; Stagg et al., 2011; Buetefisch et al., 2018). It is held that the IO curve reflects the recruitment of larger neuronal populations at increased TMS intensities, but also a change in balance between GABAergic and glutamatergic activity within M1 (Chen, 2000; Boroojerdi et al., 2001; Möller et al., 2009).

Lastly, SICI and ICF reflect M1 intracortical mechanisms that can be tested using ppTMS over M1. The SICI effect consists of a reduction in MEP size that is obtained when a suprathreshold test TMS pulse over M1 is preceded by a subthreshold conditioning TMS pulse administered with the same coil at short (i.e., 1–5 ms) ISIs. The ICF effect consists of an increase in MEP size that is obtained when conditioning and test pulses are administered with longer ISIs (i.e., 7–20 ms). Studies indicate that these inhibitory (SICI) and facilitatory (ICF) modulations of MEP amplitude take place at the cortical level without affecting spinal circuits (Kujirai et al., 1993; Ziemann et al., 1996; Schwenkreis et al., 2000; Peurala et al., 2008; Tandonnet et al., 2010). SICI is classically thought to represent the activation of populations of inhibitory interneurons reflecting $GABA_A$ transmission; ICF, on the other hand, is a more complex measure generally considered a proxy of N-methyl-D-aspartate (NMDA) glutamatergic interneurons within M1 (Kujirai et al., 1993; Ziemann et al., 1996a, 1998; Liepert et al., 1997; Di Lazzaro et al., 2000; Paulus et al., 2008).

Consistent with the concepts of Hebbian plasticity and STDP (Hebb, 1949; Jackson et al., 2006; Caporale and Dan, 2008; Markram et al., 2011; Romei et al., 2016b) and prior ccPAS work (Buch et al., 2011; Koch et al., 2013; Romei et al., 2016a) $ccPAS_{PMv\rightarrow M1}$ would lead to LTP of PMv-to-M1 projections. If the protocol potentiates PMv-to-M1 excitatory interactions via synaptic plasticity, we expect that $ccPAS_{PMv\rightarrow M1}$ aftereffects could be traceable locally at the level of M1 intracortical circuitry, as M1 neurons might be affected by the increased efficacy of PMv excitatory inputs into them. In turn, this would result in increased M1 corticospinal excitability assessed through spTMS and evidenced by reduced rMT and SI_{1mV} and steeper IO recruitment curves. Investigating SICI and ICF allowed us to test for potentiated PMv-to-M1 projections due to $ccPAS_{PMv\rightarrow M1}$ effects on GABAergic and glutamatergic transmission in M1, which is key to synaptic plasticity (Jacobs and Donoghue, 1991; Hess and Donoghue, 1996; Ziemann et al., 2001; Rosenkranz and Rothwell, 2006). Importantly, assessing the activity of inhibitory and excitatory interneurons projecting to M1 corticospinal neurons provides novel mechanistic insights into the physiological basis of ccPAS and its impact on corticospinal output.

2. Materials and methods

2.1. Participants

A total of 60 right-handed healthy volunteers took part in the study. 15 participants (8 females, mean age ± standard deviation: 23 ± 2.5 years) were tested in a pilot study whose aim was to provide insights into PMv-to-M1 interactions underlying the ccPAS protocol and select the most promising ISI (see below). In the main experiment, participants were randomly assigned to two groups of 24 individuals each, one undergoing $ccPAS_{PMv\rightarrow M1}$ and the other $ccPAS_{M1\rightarrow PMv}$. Three participants were tested in both groups, with the two sessions at least three weeks apart. The two groups were balanced for age and gender (see Table 1). Before starting the experiment, all participants gave informed consent and were screened to avoid adverse reactions to TMS (Rossini et al., 2015; Rossi et al., 2021). All the experimental procedures were performed in accordance with the 1964 Declaration of Helsinki and later amendments (WMA, 2013), and approved by the Department of Psychology "Renzo Canestrari" Ethical Committee and the Bioethics Committee at the University of Bologna. During the experiment the recommended safety procedures for non-invasive brain stimulation during the COVID-19 pandemic were followed (Bikson et al., 2020). No adverse reactions or TMS-related discomfort were reported by participants or noticed by the experimenters.

Table 1
Demographic characteristics of participants in the main experiment. Chi-square and F tests were performed to ensure there were no differences in gender or age across groups.

	Gender	Age (mean ± standard deviation)
$ccPAS_{PMv\rightarrow M1}$	$F = 15$	22.67 $y \pm 3.22$
group	$M = 9$	22.89 $y \pm 2.15$
$ccPAS_{M1\rightarrow PMv}$	$F = 12$	22.58 $y \pm 2.50$
group	$M = 12$	24.42 $y \pm 3.96$
Statistical analysis	X^2 =0.76; $p = 0.38$	All $F \leq 1.27$; all $p \geq .26$

2.2. Pilot dual coil TMS study

The purpose of the pilot study was to select the best ISI for testing short-latency effective connectivity from PMv to M1 in young healthy adults using dual coil TMS (Rossini et al., 2015; Davare et al., 2008, 2009; Fiori et al., 2016; 2017; Chiappini et al., 2020), to inform the ccPAS protocol to be used in the main experiment. We therefore explored the effect of PMv conditioning on M1 excitability by varying the ISI between the two TMS pulses (6, 8 and 10 ms ISIs). PMv was stimulated at a subthreshold intensity (90% of the individual rMT; see below), whereas M1 was stimulated at a suprathreshold intensity necessary to induce MEPs of ~1 mV of amplitude (SI_{1mv}). We derived stimulation parameters from our prior $ccPAS_{PMv\rightarrow M1}$ studies (Fiori et al., 2018; Turrini et al., 2022, 2023), which were also used in the main experiment. See Supplementary Materials for details on the pilot study and below for details on the main experiment.

2.3. General experimental design

The main study aimed to assess the neurophysiological effects of ccPAS on motor excitability. To this end, each participant underwent a neurophysiological assessment consisting of rMT, SI_{1mV}, IO curve, SICI and ICF measures in two test blocks: one before (Pre) and one immediately after (Post) the administration of ccPAS (Fig. 1). We first determined the rMT, followed by the SI_{1mV}. Then, the order of the other measures (IO curve, SICI and ICF) was counterbalanced across participants, but remained constant for each individual between the Pre and Post block.

We delivered two ccPAS protocols to manipulate the strength of the pathway between the left PMv and left M1 (Buch et al., 2011; Johnen et al., 2015; Fiori et al., 2018; Chiappini et al., 2020; Sel et al., 2021). For participants assigned to the $ccPAS_{PMv\rightarrow M1}$ group, during the ccPAS, the pulse over PMv always preceded that over M1; for those assigned to the group $ccPAS_{M1\rightarrow PMv}$, instead, the order was reversed and PMv stimulation always followed M1 stimulation. During these protocols, we recorded MEPs to test for online changes in motor system excitability (Fiori et al., 2018; Turrini et al., 2022, 2023). Moreover, before (Pre) and after (Post) the ccPAS protocol, participants underwent neurophysiological assessment (Fig. 1).

2.4. Neurophysiological assessment

Ag/AgCl surface electrodes were placed in a belly-tendon montage over the right first dorsal interosseus muscle (FDI). EMG signals were acquired using a Biopac MP-35 (Biopac, U.S.A.) electromyograph, band-pass filtered between 30 and 500 Hz and sampled at 10 kHz. TMS was performed using a Magstim Bistim^2 stimulator composed of two Magstim 200^2 units (The Magstim Company, Carmarthenshire, Wales, U.K.). During the test blocks the two Magstim 200^2 units were combined through a connecting module so that ppTMS and spTMS were delivered though a 50-mm iron branding figure-of-eight coil (Fig. 2a,b). Pulses were remotely triggered by a MATLAB script (The MathWorks, Natick, USA).

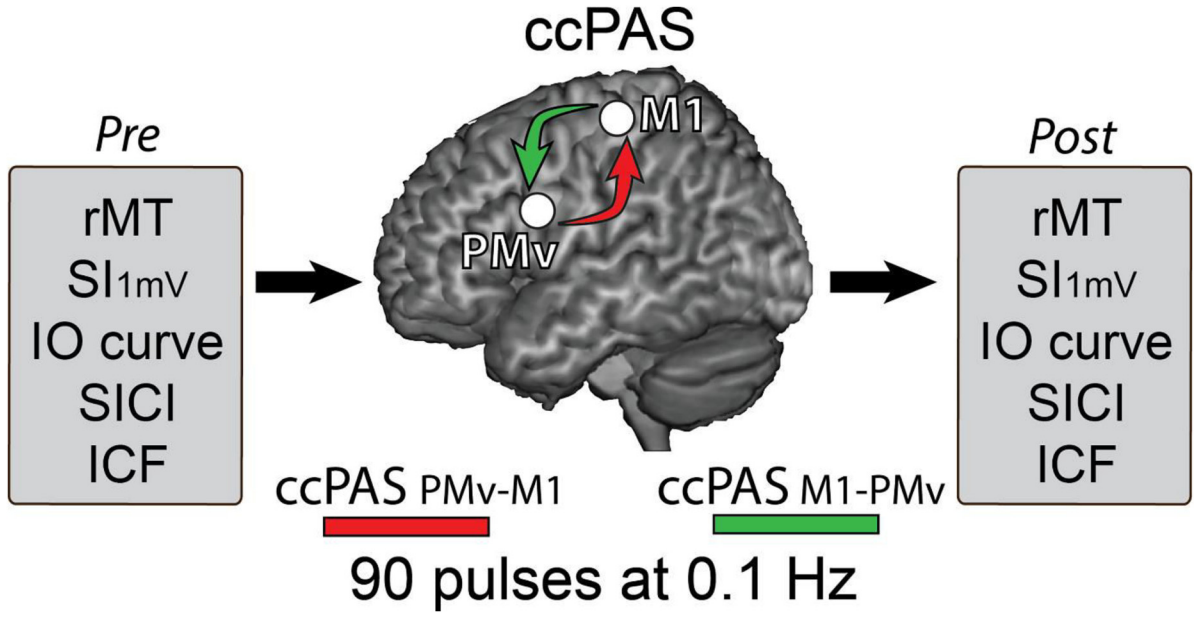

Fig. 1. General experimental design. rMT, SI_{1mV}, the IO curve, and intracortical parameters SICI and ICF were assessed before and after a plasticity induction period consisting of 90 pairs of pulses delivered at 0.1 Hz over the ventral premotor-to-motor circuit. In the $ccPAS_{PMv \rightarrow M1}$ group the stimulation over PMv always preceded the M1 pulse by 8 ms; conversely, in the $ccPAS_{M1 \rightarrow PMv}$, PMv always followed M1 stimulation by 8 ms.

The experiment started with the electrode montage setup. Then, we localized the left M1 as the optimal scalp position where MEPs of maximal amplitudes could be induced in the right FDI and the localization of the left PMv using neuronavigation (see below). The coil over left M1 was positioned tangentially to the scalp at an angle of 45° from the midline to induce a posterior-to-anterior current in the brain (Kammer et al., 2001; Di Lazzaro et al., 2004), and was used for testing all indices in the Pre and Post blocks.

Both blocks started with assessment of the rMT, defined as the minimum intensity of stimulator output that evokes MEPs with an amplitude of at least 50 μV in 5 out of 10 consecutive trials (Rossini et al., 1994). Then, we assessed the intensity required to obtain MEPs of an average peak-to-peak amplitude of 1 mV (SI_{1mV}).

The rMT and SI_{1mV} were reassessed following the ccPAS, and the intensity parameters of all other indices (i.e., the IO curve, and conditioning and test stimulus intensities for SICI and ICF) were readjusted accordingly (Kujirai et al., 1993; Sanger et al., 2001; Cirillo et al., 2009; Lu et al., 2012; Singh et al., 2014; Murase et al., 2015). For the IO curve, 10 MEPs were collected at each intensity ranging from 100% to 150% of the rMT in steps of 10% (60 trials total). SICI and ICF (30 trials each) were recorded in accordance with established protocols (Kujirai et al., 1993; Ziemann et al., 1996). They consisted of paired TMS pulses (ppTMS) delivered through the same coil over the left M1. The first stimulus was labeled the conditioning stimulus and preceded the test stimulus by 3 ms for SICI and 12 ms for ICF (Borgomaneri et al., 2015a, 2015b, 2017). The intensity of the conditioning stimulus was set to 80% of rMT, while the test stimulus intensity was set to SI_{1mV}. 30 MEPs induced by the test stimulus alone (spTMS) were also separately recorded. To minimize carryover effects, for all three indices (IO curve, SICI, ICF) the trials were separated by a random time ranging from 6430 to 8570 ms.

2.5. ccPAS protocol

The ccPAS consisted of 15 min of paired pulses delivered over the left PMv and M1 sites at 0.1 Hz (i.e., 90 paired pulses), with an ISI of 8 ms (Buch et al., 2011; Johnen et al., 2015; Fiori et al., 2018; Chiappini et al., 2020; Sel et al., 2021), to activate short latency connections between the two areas (Davare et al., 2008, 2009). During ccPAS administration, the two Magstim 200^2 units were separate so to administer TMS over two distinct areas with two distinct 50-mm iron branding figure-of-eight coils, with the handles perpendicular to the plane of the wings to minimize their interference in the paired stimulation of PMv and M1 during ccPAS (Fig. 2a,b). To calibrate ccPAS stimulation intensity, before protocol administration we reassessed rMT and SI_{1mV} using the configuration with two separate Magstim units. The coil over left M1 was placed as previously described, and M1 was stimulated with an intensity equal to SI_{1mV}. The PMv coil was placed tangentially to the scalp, inducing a current flow in the neural tissue pointing toward the M1 site (Buch et al., 2011; Johnen et al., 2015; Fiori et al., 2018; Fig. 2a,b). PMv stimulation intensity was adjusted to 90% of each participant's rMT (Fiori et al., 2018; Chiappini et al., 2020; Turrini et al., 2022, 2023). The effectiveness of subthreshold conditioning has been demonstrated in other ccPAS studies (Koch et al., 2013; Fiori et al., 2018; Chiappini et al., 2020; Turrini et al., 2022, 2023) and is also supported by dcTMS studies testing PMv-to-M1 interactions (Davare et al., 2008, 2009; Bäumer et al., 2009; Fiori et al., 2016, 2017). To minimize potential discomfort, we exposed participants to active stimulation of PMv beforehand, using 3, 4 pulses of increasing intensity. All participants tolerated the stimulation well.

2.6. Neuronavigation

The left PMv was identified using a SofTaxic Navigator System (Electro Medical System, Bologna, IT), as in previous studies conducted in our laboratory (Avenanti et al., 2013a; Tidoni et al., 2013; Valchev et al., 2017). Skull landmarks (2 preauricular points, nasion and inion) and ~80 points were digitized using a Polaris Vicra digitizer (Northern Digital). We obtained an estimated MRI through a 3D warping procedure fitting a high-resolution MRI template to each participant's scalp and craniometric points. To target the left PMv, we used the following Talairach coordinates: $x = -52$; $y = 10$; $z = 24$. These coordinates were obtained by averaging the coordinates reported in previous studies (Davare et al., 2006; Dafotakis et al., 2008; Avenanti et al., 2012, 2018; Jacquet and Avenanti, 2015); those studies showed that stimulating this ventral frontal site (at the border between the anterior sector of the PMv and the posterior sector of the inferior frontal gyrus) affected planning, execution and perception of hand actions. These coordinates

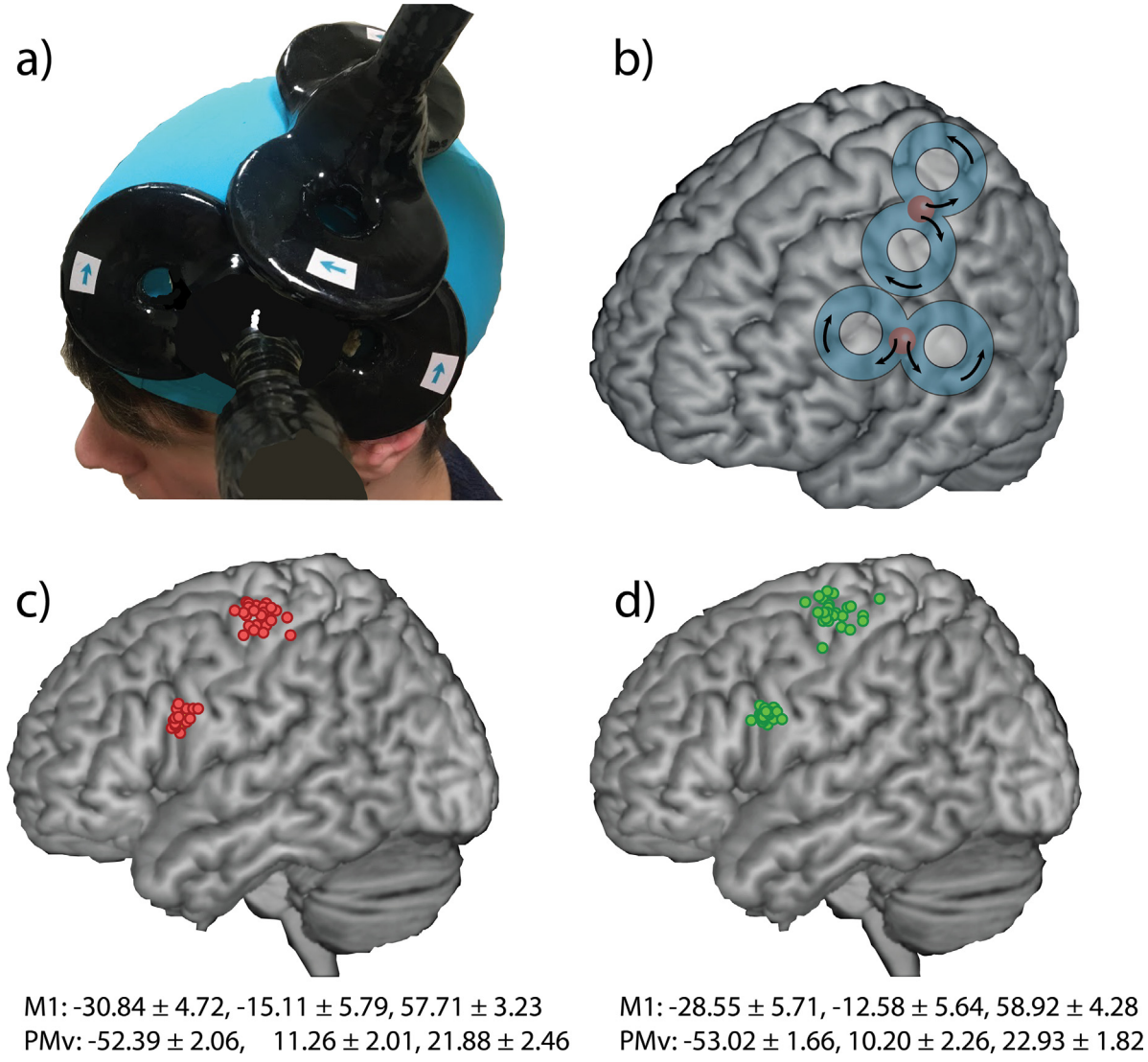

Fig. 2. (a) Coil positioning on the scalp. (b) Coils' location and orientation; the arrows indicate current directions within the coils. (c) and (d) Individual targeted sites reconstructed on a standard template using MRIcron software after conversion to MNI space for illustrative purposes. (c) $ccPAS_{PMv \rightarrow M1}$ group. (d) $ccPAS_{M1 \rightarrow PMv}$ group.

are also consistent with those used in previous ccPAS (Buch et al., 2011; Johnen et al., 2015; Fiori et al., 2018; Chiappini et al., 2020), TMS-EEG (Zanon et al., 2018) and dual-site TMS studies targeting PMv-to-M1 connections (Davare et al., 2008, 2009; Fiori et al., 2016, 2017). The Talairach coordinates corresponding to the projections of the left PMv and M1 scalp sites onto the brain surface were estimated by the SofTaxic Navigator from the MRI-constructed stereotaxic template, and the resulting coordinates are consistent with the regions defined as human PMv and M1 (Mayka et al., 2006; Fig. 2c,d).

2.7. Data preprocessing

All data were processed offline. MEP peak-to-peak amplitudes were measured within a 60-ms time-window starting 15 ms after the test stimulus, using a MATLAB script. Since background EMG affects motor excitability (Devanne et al., 1997), we discarded any MEP showing EMG activity in the preceding 100-ms time-window that deviated from the individual mean of the block by more than 2 SD; moreover, we discarded outlier MEPs deviating from the mean amplitude of their test block by more than 3 SD (6% of MEPs excluded in total). (For further data preprocessing in the pilot study, see Supplementary Materials.) In the Main Experiment, each participant's IO curve was assessed by plotting the mean MEP amplitude vs. the intensity of stimulation; the data were subsequently fitted with a sigmoid function equation (Houdayer et al., 2008; Kemlin et al., 2019): $MEP(s) = MEP_{max}/(1 + \exp^{m(IP-s)})$, where MEP(s) is the MEP amplitude at the stimulation intensity s, MEP_{max} is the upper asymptote, IP is the inflection point, and m is the global slope of the function. From these parameters, we also derived the curve's peak slope (PS), which is the instantaneous slope of the ascending limb of the curve at the steepest point, reflecting the recruitment gain of motoneurons (Kemlin et al., 2019). PS is calculated using the following formula: $PS = m \times MEP_{max}/4$. SICI and ICF indices were expressed as the ratio between MEP amplitudes induced by ppTMS (conditioned and test pulse) and spTMS (test pulse alone). As expected, considering the widely reported individual variability in SICI (Chen, 2004; Caranzano et al., 2017), 4 participants (2 per group) did not show an inhibitory effect using the chosen protocol; rather, these participants showed a marked facilitation (mean +1.73) and were statistical outliers deviating from the mean of their group by over 2 SD. To ensure that changes in SICI between conditions were not obscured by floor effects (Fisher et al., 2002), these participants were excluded from the main analysis of SICI reported in the main text (Sinclair and Hammond, 2009). Yet, in a further anal-

ysis all participants were included (see Supplementary Results). 2 participants belonging to the $ccPAS_{M1\rightarrow PMv}$ group were excluded from the analysis of MEPs collected during the ccPAS, due to a technical failure.

2.8. Statistical analyses

Data normality was assessed by visual inspection and using the Shapiro-Wilk test. Parametric and non-parametric analyses were chosen accordingly. In the Main Experiment, rMT and SI_{1mV} data were normally distributed. Therefore, we ran two separate mixed factors ANOVAs, one for each index, with the within-subjects factor Time (2 levels: Pre and Post block) and the between-subjects factor Group (2 levels: $ccPAS_{PMv-M1}$ and $ccPAS_{M1\text{-}PMv}$). Data collected during the ccPAS were also normally distributed and were therefore analyzed using an ANOVA by dividing the 90 pulses into 6 epochs of 15 MEPs each (Fiori et al., 2018); the resulting analysis included the factors Epoch (within, 6 levels) and Group (between, 2 levels: $ccPAS_{PMv-M1}$ and $ccPAS_{M1\text{-}PMv}$). Newman Keuls post-hoc analyses were performed to correct for multiple comparisons. In all the ANOVAs, partial η^2 ($\eta_p{}^2$) was computed as a measure of effect size for significant main effects and interactions. For significant post-hoc comparisons, Cohen's *d* was computed. By convention, $\eta_p{}^2$ *effect* sizes of ~ 0.01, ~.06, and ~.14 are considered small, medium and large, respectively. Cohen's *d* effect sizes of ~.2, ~.5, ~.8 are considered small, medium and large instead (Cohen, 1992).

All parameters obtained from fitting IO curves, i.e., the slope, asymptote, inflection point and peak slope, as well as SICI and ICF data were not normally distributed, so direct comparisons between and within groups were computed through nonparametric Mann Whitney U and Wilcoxon signed-rank tests, respectively. All the analyses were conducted using STATISTICA (version 12, StatSoft, Tulsa, USA).

3. Results

3.1. dcTMS highlights early facilitatory PMv-to-M1 interactions

The pilot study confirmed that an 8-ms ISI is best suited to consistently influence M1 excitability via PMv conditioning (Buch et al., 2011; Davare et al., 2008, 2009; Fig. S1). Interestingly, we observed that PMv conditioning over MEPs induced by M1 stimulation was facilitatory, i.e., PMv conditioning increased M1 corticospinal excitability when the ISI was set at 8 ms (Fig. S1 and Supplementary Results for details). This provides insights into the physiological basis of the ccPAS protocol used in the main experiment.

3.2. Enhancement of MEPs during $ccPAS_{PMv\rightarrow M1}$ administration

In the main study, MEPs recorded during the ccPAS protocols (i.e., 90 MEPs for each protocol, one for each paired stimulation of PMv and M1) were analyzed by means of an Epoch x Group ANOVA which showed a significant main effect of Epoch ($F_{5,220} = 8.58$, $p < .001$; $\eta_p{}^2 = 0.16$) and an Epoch x Group interaction ($F_{5,220} = 2.85$, $p = .02$; $\eta_p{}^2 = 0.06$), suggesting that the average MEP amplitude varied differently according to the ccPAS protocol being administered (Fig. 3a). Newman-Keuls post-hoc analyses further clarified the interaction: the $ccPAS_{PMv\rightarrow M1}$ group showed an increase in MEP amplitude over epochs, almost significant in the second compared to the first ($p = .06$, *Cohen's d* = 0.67), and fully significant from the third to the sixth (all $p \leq 0.004$; all *Cohen's d* ≥ 0.76). No change in MEP amplitude was detected in the $ccPAS_{M1\rightarrow PMv}$ group across epochs (all $p \geq .09$). This effect was further explored by extracting a MEP modulation index, computed as the difference between MEP amplitude in Epoch 6 and Epoch 1 of the ccPAS, and comparing that index between the two groups (Fig. 3d); the analysis revealed a significant difference between the two groups (t_{44}=2.88, $p = .006$; *Cohen's d* = 0.86), indicating a greater modulation during $ccPAS_{PMv\rightarrow M1}$ compared to $ccPAS_{M1\rightarrow PMv}$.

3.3. Reduction in rMT and SI_{1mV} following $ccPAS_{PMv\rightarrow M1}$

The Time x Group ANOVA conducted on rMT showed no main effect of Time or Group (all $F \leq 2.90$, $p \geq .10$), but a significant Time x Group interaction ($F_{1,46} = 5.07$, $p = .03$; $\eta_p{}^2$=0.10; Fig. 4a), suggesting that rMT varied differently over time based on the administered ccPAS protocol. Newman-Keuls post-hoc analyses revealed that rMT was comparable between the two groups at baseline ($p = .75$). Following the plasticity induction, the $ccPAS_{PMv\rightarrow M1}$ group showed a significant decrease in rMT ($p = .008$, *Cohen's d* = 0.64; Fig. 4a, top row), while no change was detected for the $ccPAS_{M1\rightarrow PMv}$ group ($p = .70$; Fig. 4a, middle row). This effect was further qualified by an analysis conducted on an rMT modulation index computed as the difference between rMT in the Post and Pre blocks; the modulation index was significantly different between the two groups ($t_{46} = -2.25$, $p = .029$; *Cohen's d* = 0.65; Fig. 4a, bottom row).

Similar effects were detected in the ANOVA conducted on SI_{1mV}: a significant main effect of Time ($F_{1,46} = 4.93$, $p = .03$; $\eta_p{}^2 = 0.10$) was qualified by a significant Time x Group interaction ($F_{1,46} = 6.81$, $p = .01$; $\eta_p{}^2$=0.13; Fig. 4b), which was explored through post-hoc analyses. The SI_{1mV} intensities were comparable at baseline ($p = .30$) and decreased following $ccPAS_{PMV\rightarrow M1}$ ($p = .001$, *Cohen's d* = 0.59; Fig. 4b, top row), but not after $ccPAS_{M1\rightarrow PMv}$ ($p = .92$; Fig. 4b, middle row). A SI_{1mV} modulation index was calculated as the difference between SI_{1mV} in the Post and Pre blocks and compared between the two groups, revealing a significant difference (t_{46}=–2.61; p=.012; *Cohen's d* = 0.75; Fig. 4b, bottom row).

3.4. Enhancement of IO curve following $ccPAS_{PMv\rightarrow M1}$

Fig. 5 shows a steeper IO curve following $ccPAS_{PMv\rightarrow M1}$, but not following $ccPAS_{M1\rightarrow PMv}$. Mann-Whitney comparisons conducted on IO curve parameters, namely the slope, the MEP_{max} (upper asymptote) and the inflection point, showed no differences between groups at baseline (all $p \geq .14$). Wilcoxon paired samples tests showed that the slope parameter significantly increased in the Post block compared to the Pre block only in the $ccPAS_{PMv\rightarrow M1}$ group (mean ± standard deviation: 10.77 ± 3.81 vs. 16.76 ± 9.61; $p = .03$, Fig. 5a). In contrast, no change was observed in the $ccPAS_{M1\rightarrow PMv}$ group (12.95 ± 5.46 vs. 14.49 ± 7.58; $p = .48$, Fig. 5b). Similar results, although only marginally significant, were also obtained for the inflection point: its value decreased (i.e., the curve shifted to the left, suggesting that higher MEPs could be obtained with lower stimulation intensities) in the $ccPAS_{PMv\rightarrow M1}$ group (1.30 ± 0.13 vs. 1.23 ± 0.08; $p = .059$; Fig. 5a), but not in the $ccPAS_{M1\rightarrow PMv}$ group (1.29 ± 0.18 vs. 1.22 ± 0.06; $p = .10$). In contrast, the asymptote was not affected by the applied protocol (both $p \geq .35$). However, the peak slope parameter (PS), which is calculated from both the slope and the upper asymptote, was differentially impacted by the administered ccPAS protocol. Indeed, it increased only after $ccPAS_{PMv\rightarrow M1}$ (6.87 ± 5.78 vs. 9.98 ± 11.61; $p = .004$), but not $ccPAS_{M1\rightarrow PMv}$ (10.27 ± 6.52 vs. 10.14 ± 7.88; $p = .65$). See Fig. S2 for further analyses.

3.5. Reduction of SICI, but not of ICF, following $ccPAS_{PMv\rightarrow M1}$

As previously stated, mean MEP amplitudes elicited by the test stimulus alone (spTMS) should not differ across timepoints as SI_{1mV} intensity was reassessed following ccPAS. In keeping with this, the Time x Group ANOVA conducted on these MEPs revealed no significant main effects nor interactions (all $F \leq 2.48$; all $p \geq .12$).

A non-parametric comparison using a Mann-Whitney test found no differences in SICI between groups at baseline ($p = .20$). Intracortical inhibition was differentially impacted by the two ccPAS protocols, as shown by Wilcoxon tests: the inhibitory effect decreased following $ccPAS_{PMv\rightarrow M1}$ ($p = .03$, Fig. 6a, top row) and showed a non-significant

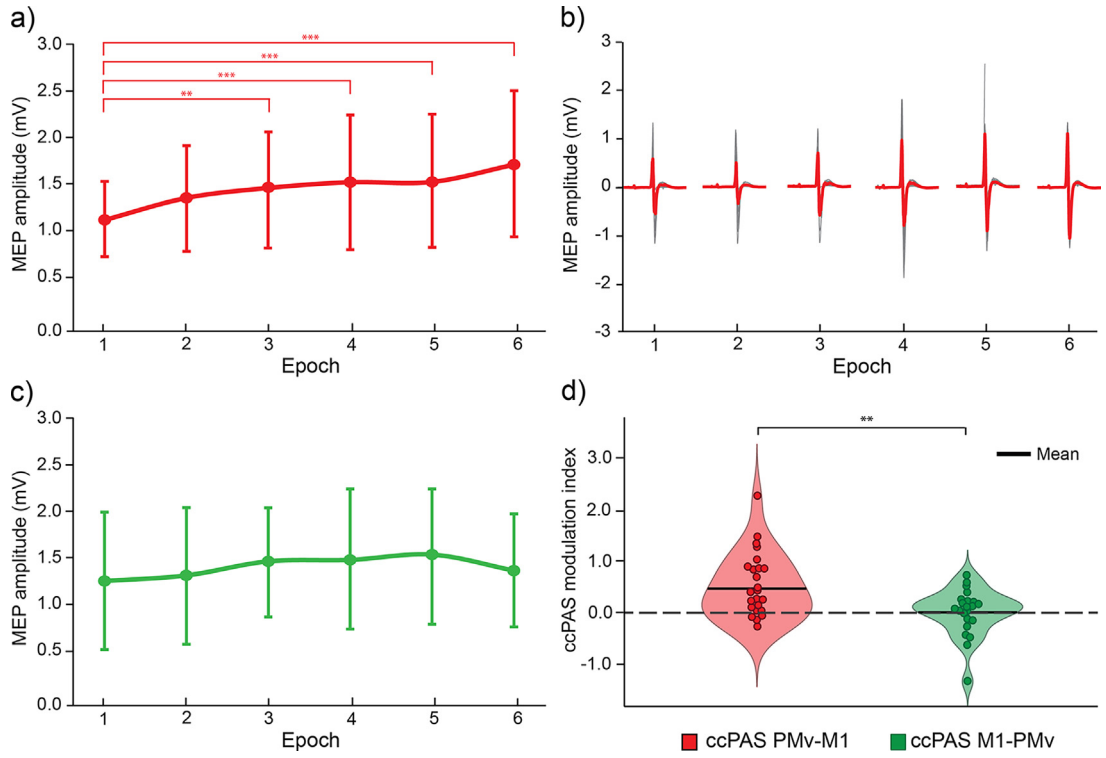

Fig. 3. (a) MEP amplitudes collected during $ccPAS_{PMv \rightarrow M1}$ (red line, $N = 24$). (b) Example of EMG traces from one representative participant during the $ccPAS_{PMV \rightarrow M1}$ protocol; gray and red superimposed lines represent single trial EMG traces and median MEP EMG traces, respectively. (c) Average MEP amplitude collected during the ccPAS protocol in the $ccPAS_{M1 \rightarrow PMv}$ group (green line, $N = 22$). (d) Violin plots showing individual MEP modulation during the ccPAS, computed as the difference between MEP amplitudes in Epoch 6 and Epoch 1, in both groups. Asterisks indicate significant comparisons (** $p \leq 0.01$, *** $p \leq 0.001$). Error bars represent one standard deviation.

increase following $ccPAS_{M1 \rightarrow PMv}$ ($p = .12$, Fig. 6a, middle row). The differential effect of the two ccPAS protocols on intracortical inhibition was further corroborated by extracting a SICI modulation index, computed as the difference between SICI in the Post and Pre blocks. Direct comparison revealed a significant difference ($p = .012$) between the two groups (Fig. 6a, bottom row). The same analyses conducted on ICF found no baseline differences between groups ($p = .35$), and no difference across time points in either group (both $p \geq .15$). To minimize the influence of statistical outliers, in a further analysis we used modified SICI index on the entire sample of participants (Fig. S3). The analysis replicated the main findings reported in Fig. 6 and showed also a significant increase in SICI following $ccPAS_{M1 \rightarrow PMv}$. See Supplementary material for further discussion.

4. Discussion

Although several studies have applied ccPAS to enhance PMv-to-M1 connectivity via Hebbian plasticity (Buch et al., 2011; Johnen et al., 2015; Fiori et al., 2018; Sel et al., 2021; Turrini et al., 2022, 2023), prior work did not systematically investigate ccPAS effects on M1 corticospinal excitability or intracortical mechanisms in M1, leaving the question of whether ccPAS acts locally over M1 unclear. To answer this question, in the present study we tested: i) online changes in motor excitability probed by dcTMS of PMv and M1 during ccPAS administration; ii) ccPAS aftereffects on multiple indices of M1 corticospinal excitability; and iii) ccPAS aftereffects on distinct populations of intracortical inhibitory and facilitatory interneurons. Our study provides evidence that $ccPAS_{PMv \rightarrow M1}$ enhances distinct indices of M1 corticospinal excitability and suppresses inhibitory interneuronal activity, thus demonstrating local changes in M1 that are relevant for understanding the physiological bases of ccPAS.

Building on prior work (Buch et al., 2011; Johnen et al., 2015; Fiori et al., 2018; Sel et al., 2021; Turrini et al., 2022, 2023) and a dcTMS pilot study, we applied a ccPAS protocol using a short ISI (8 ms) between the pulses, targeting a cortico-cortical route between the two sites (Davare et al., 2008, 2009). Our dcTMS pilot study showed that subthreshold PMv conditioning tends to already increase M1 corticospinal excitability at a 6-ms ISI, but the most consistent facilitation was observed at an 8-ms ISI (Fig. S1). Therefore, by adopting the latter ISI in our $ccPAS_{PMv \rightarrow M1}$ protocol, we assumed that, in each TMS pair, the corticocortical volley elicited by PMv stimulation reached M1 immediately before the pulse over M1, resulting in convergent activation of pre- and post-synaptic neural populations in M1. This is instrumental to the establishment of Hebbian STDP plasticity in the PMv-to-M1 pathway (Buch et al., 2011; Chiappini et al., 2020; Sel et al., 2021; Turrini et al., 2022, 2023). In the main experiment, these facilitatory PMv-to-M1 interactions were thus coherently and repeatedly elicited in the critical $ccPAS_{PMv \rightarrow M1}$ condition to induce LTP in PMv-to-M1 connections.

The most novel finding of our study is the robust and convergent evidence of enhanced M1 corticospinal excitability following $ccPAS_{PMv \rightarrow M1}$, supporting LTP-like effects within the targeted motor circuit (Buch et al., 2011; Koch et al., 2013; Romei et al., 2016b). First, in keeping with our prior studies (Fiori et al., 2018; Turrini et al., 2022, 2023), we observed that the repeated paired stimulation of PMv and M1 during $ccPAS_{PMv \rightarrow M1}$ caused a gradual increase in MEP amplitude – showing a progressive build-up of functional plasticity that already begins during protocol administration. In line with prior research focused on changes in PMv-to-M1 connectivity (Buch et al., 2011; Chiappini et al., 2020), it is likely this gradual increase primarily reflects LTP of the PMv-to-M1 pathway, increasing the efficacy of PMv synaptic input to M1 interneurons, which in turn shape the output of pyramidal cells (see below). Second, consistent with these online changes, we observed further potentiation effects on M1 corticospinal neurons af-

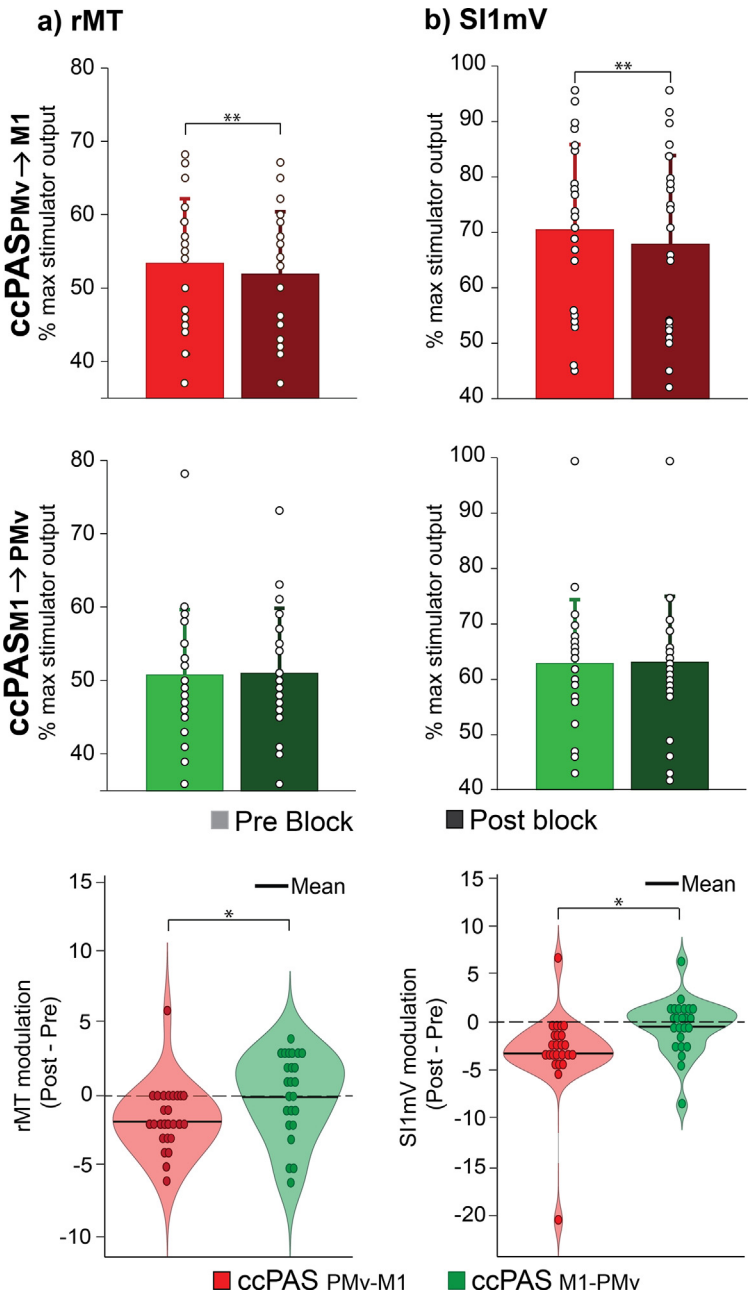

Fig. 4. Effects of ccPAS on (a) rMT and (b) SI_{1mV}. The top row depicts motor thresholds before (lighter bars) and after (darker bars) the $ccPAS_{PMV→M1}$ protocol ($N = 24$); the middle row depicts motor thresholds before (lighter bars) and after (darker bars) the $ccPAS_{M1→PMv}$ protocol ($N = 24$); the bottom row depicts violin plots showing individual modulation in motor thresholds, computed as the difference between rMT (a) and SI_{1mV} (b) in the Post and Pre blocks, in both groups. Asterisks indicate significant comparisons ($^{*}p \leq 0.05$; $^{**}p \leq 0.01$). Error bars represent one standard deviation.

ter ccPAS administration. Following $ccPAS_{PMv→M1}$ we found a decrease in both the rMT and the intensity necessary to produce MEPs of 1-mV amplitude (SI_{1mV}), indicating a shift towards increased excitability of both lower- and higher-threshold M1 corticospinal neurons. This was also accompanied by a steeper IO curve as shown by changes in the slope and the peak slope, and marginal changes in inflection point; remarkably, IO curve changes were detected despite having re-adjusted all stimulation intensities with respect to the re-assessed rMT in the Post block. Because rMT decreased following $ccPAS_{PMv→M1}$, stimulation intensities used to assess the IO curve in the Post block were lower than those used in the Pre block; nonetheless, we could still observe robust IO curve changes, reflecting greater recruitment of M1 corticospinal neurons. All these modulations were specific to the $ccPAS_{PMv→M1}$ protocol, as they were absent following the control $ccPAS_{M1→PMv}$ condition. These changes were thus not merely due to generic stimulation of either PMv or M1, but depended on the specific manipulation of directional connectivity aimed at increasing efficacy of excitatory synaptic inputs from PMv to M1, meeting the Hebbian principle.

Taken together, changes in the rMT, SI_{1mV}, and IO curve demonstrate that ccPAS, besides strengthening PMv-to-M1 connectivity as previously demonstrated (Buch et al., 2011; Johnen et al., 2015; Chiappini et al., 2020), also acts locally by affecting descending M1 corticospinal neurons due to increased synaptic input. While previous studies that directly tested connectivity changes following ccPAS have ascribed its effects to potentiated cortico-cortical mechanisms (Buch et al., 2011; Koch et al., 2013; Johnen et al., 2015; Santarnecchi et al., 2018), our study is the first to highlight that potentiated PMv-to-M1 projections result in a clear enhancement of M1 corticospinal excitability, which could in principle contribute to improved hand functioning following this stimulation protocol (Fiori et al., 2018; Turrini et al., 2023).

What mechanism underlies the physiological changes induced by $ccPAS_{PMv→M1}$? Research using dcTMS has shown that the premotor cortex can exert both inhibitory and excitatory influences on M1, depending on the functional state of the connection, the ISI and/or the intensity of TMS pulses (Civardi et al., 2001; Davare et al., 2008; Bäumer et al., 2009; de Beukelaar et al., 2016; Fiori et al., 2016, 2017). Based on prior

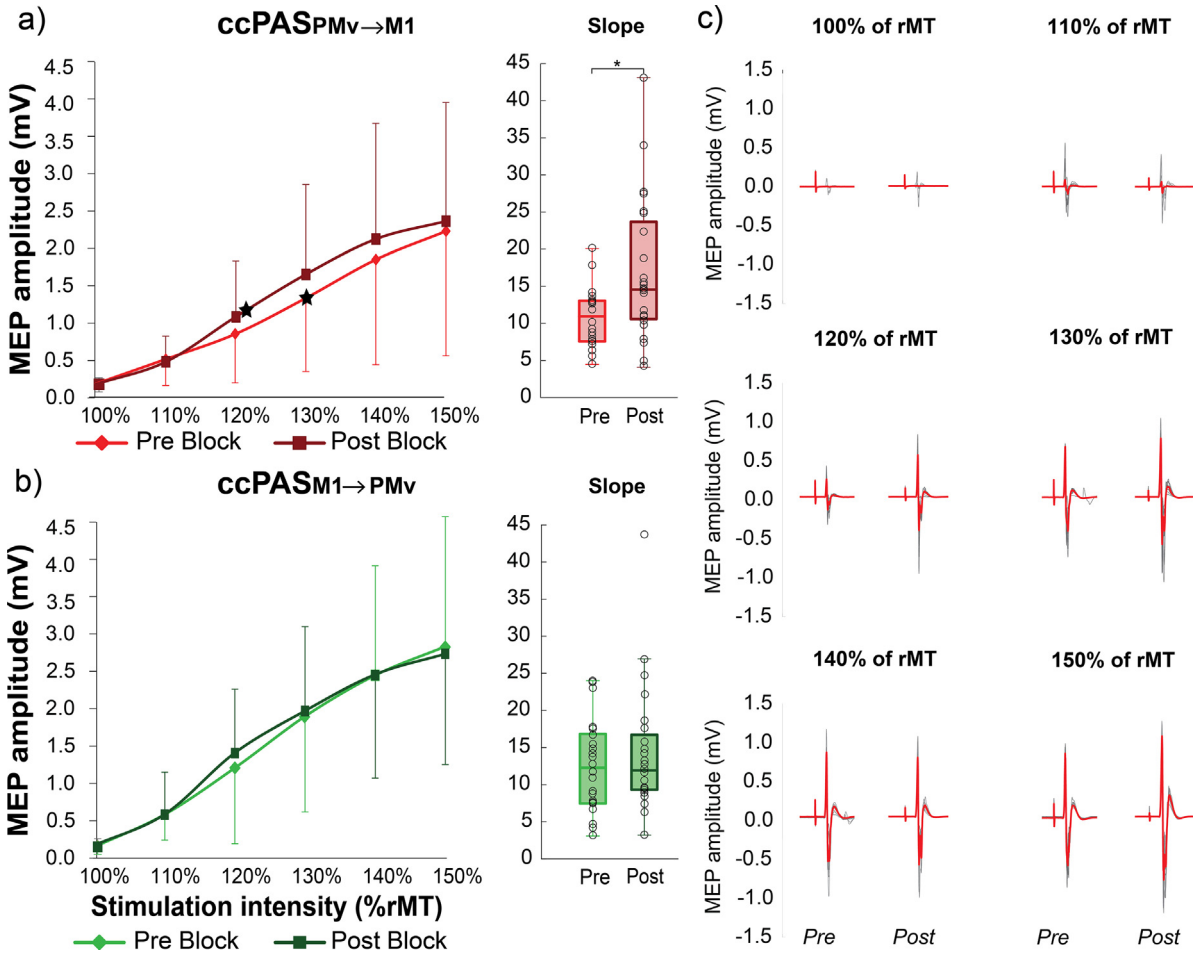

Fig. 5. Effect of ccPAS on the IO curve. (a) Effect of $ccPAS_{PMv\rightarrow M1}$, showing a steeper IO curve slope and decreased inflection points (stars) ($N = 24$). (B) Effect of $ccPAS_{PMv\rightarrow M1}$ showing no change across blocks ($N = 24$). Error bars represent one standard deviation. c) Example of IO curve EMG traces from one representative participant before and after the $ccPAS_{PMv\rightarrow M1}$ protocol. For each stimulation intensity condition of the IO curve, gray and red superimposed lines represent single trial EMG traces and median MEP EMG traces, respectively.

(e.g., Baümer et al., 2009) and present (Fig. S1) evidence of the latency of PMv-to-M1 interactions, it is arguable that the subthreshold conditioning of PMv neurons influences M1 corticospinal neurons indirectly, mainly via excitatory interneurons in M1. This fits with established anatomical and neurophysiological evidence that PMv-to-M1 projections are glutamatergic and, while a few synapse directly onto M1 corticospinal neurons, most synapse onto both glutamatergic and GABAergic M1 interneurons. These interneurons surround pyramidal cells in M1 and modulate their output, giving rise to both excitatory and inhibitory effects on corticospinal excitability ((Ghosh and Porter, 1988); Dum and Strick, 1996; Tokuno and Nambu, 2000). Neurophysiological studies in monkeys have highlighted PMv-to-M1 excitatory interactions (Ghosh and Porter, 1988; Cerri et al., 2003; Shimazu et al., 2004; Prabhu et al., 2009). These studies have shown that electrical stimulation of M1 evokes direct (D) and indirect (I_1, I_2, and I_3) volleys in the corticospinal tract, and preconditioning the PMv (monkey area F5) robustly facilitates M1 corticospinal output (Cerri et al., 2003; Shimazu et al., 2004) by acting on longer-latency I-waves (I_2 and I_3) (Shimazu et al., 2004). These later waves are generated by presynaptic inputs onto M1 corticospinal neurons (Ilić et al., 2002), suggesting that PMv conditioning can enhance excitatory interneuronal circuits within M1, which in turn impact M1 pyramidal neurons after a synaptic delay. These excitatory PMv-to-M1 interactions account for the latency and the facilitatory nature of the MEP modulations that we observed in the dcTMS pilot study, following subthreshold PMv conditioning. Similarly, during $ccPAS_{PMv\rightarrow M1}$, the repeated pairing of PMv and M1 potentiated the targeted excitatory pathway via Hebbian plasticity, increasing the efficiency of the PMv projections onto excitatory interneurons in M1. In turn, these interneurons project to pyramidal cells and contribute to regulating corticospinal excitability. During spTMS, these neural elements are likely recruited by the magnetic pulse over M1, and this explains the consistent increase in M1 corticospinal excitability following $ccPAS_{PMv\rightarrow M1}$.

Another point of novelty in our study is the finding that $ccPAS_{PMv\rightarrow M1}$ reduced the magnitude of SICI, without affecting ICF. This indicates that $ccPAS_{PMv\rightarrow M1}$ reduced local inhibitory $GABA_A$-mediated interneuronal activity within M1, which accounts for the SICI effect (Berardelli et al., 2008; Ni and Chen, 2008). A few prior studies using the classical PAS protocol have reported results similar to ours, i.e., an increase in M1 corticospinal excitability accompanied by a decrease in SICI following PAS (Kumru et al., 2017; Murase et al., 2015) or PAS combined with aerobic training (Singh et al., 2014). On the other hand, a ccPAS study targeting the parietal-motor circuit failed to observe SICI reduction and instead reported enhanced ICF (Koch et al., 2013), whereas another ccPAS study targeting cerebellar-motor circuits found a decrease in inhibition across a range of stimulation parameters (Lu et al., 2012), together with modulation of corticospinal excitability. These apparent discrepancies may reflect key features of the stimulated circuits: while parietal-to-motor connections are facilitatory (Koch et al., 2007), the cerebellum has a starkly inhibitory influence over M1 (Ugawa et al.,

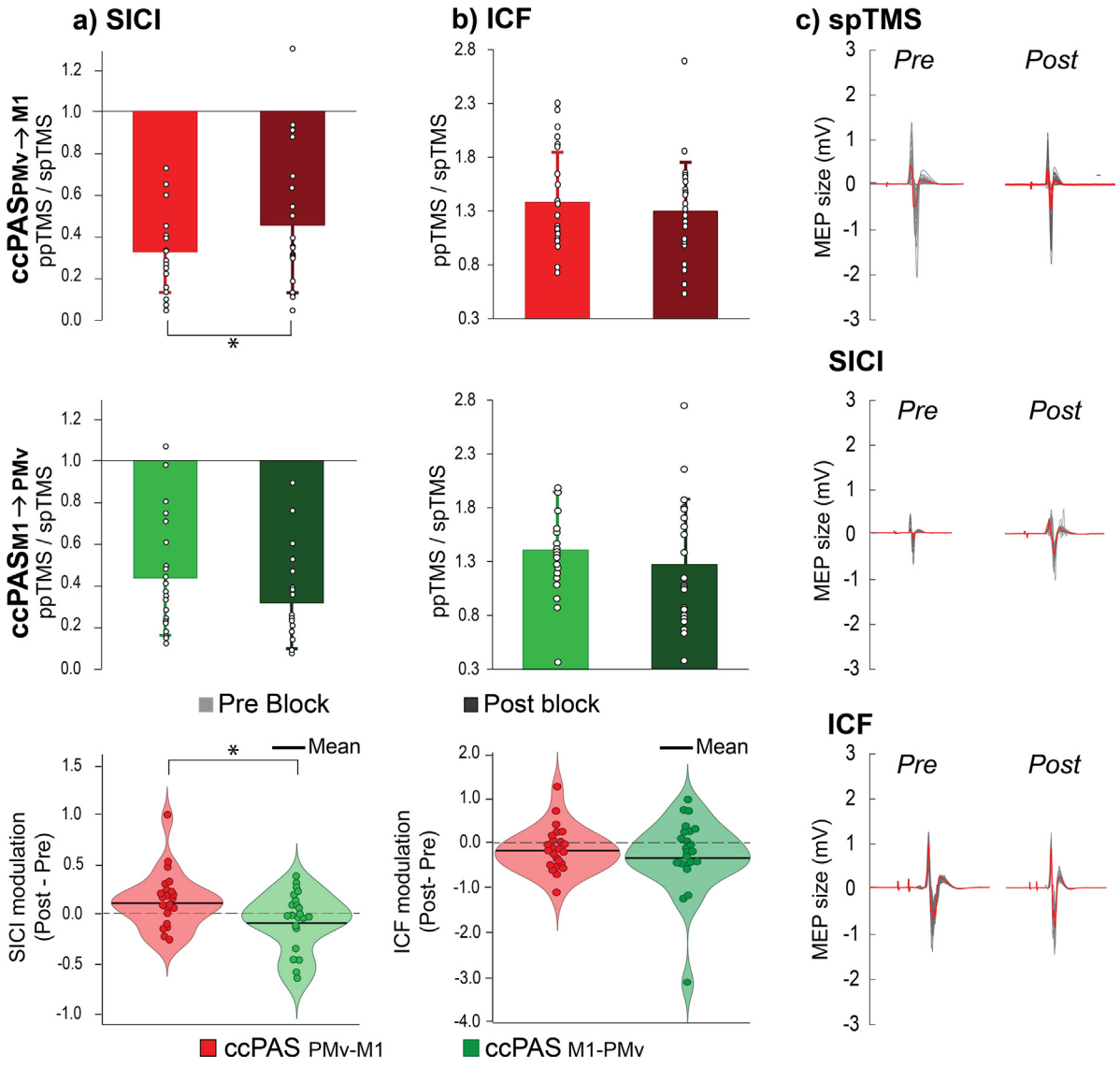

Fig. 6. Changes in intracortical inhibition (a) and facilitation (b). The top row depicts SICI and ICF before (lighter bars) and after (darker bars) the $ccPAS_{PMv\rightarrow M1}$ protocol; the middle row depicts SICI and ICF before (lighter bars) and after (darker bars) the $ccPAS_{M1\rightarrow PMv}$ protocol; the bottom row depicts violin plots showing individual modulations of SICI and ICF, computed as the difference between SICI (a) and ICF (b) in the Post and Pre blocks, in both groups. Asterisks indicate significant comparisons ($^{*}p \leq 0.05$). Error bars represent one standard deviation. (c) Example of EMG traces from one representative participant before and after the $ccPAS_{PMv\rightarrow M1}$ protocol. For each TMS condition, gray and red superimposed lines represent single trial EMG traces and median MEP EMG traces, respectively.

1995; Pinto et al., 2001). On the other hand, as reported above, the PMv exerts both facilitatory and inhibitory influences over M1 via distinct classes of interneurons.

The reduction in SICI points to a disinhibition mechanism that could contribute at least in part to the observed increase in M1 corticospinal excitability. Such a mechanisim would not contradict the notion that ccPAS induces LTP in the targeted cortico-cortical circuit (Buch et al., 2011; Koch et al., 2013; Romei et al., 2016a; Chiappini et al., 2020), or the supposed involvement of excitatory interneurons in $ccPAS_{PMv\rightarrow M1}$ as discussed above. Rather, our findings suggest that the repeated targeting of facilitatory PMv-to-M1 interactions may have biased PMv synaptic inputs toward excitatory rather than inhibitory interneurons in M1, leading to reduced $GABA_A$-mediated inhibition. This is in line with the notion of reciprocal interactions between excitatory and inhibitory processes within the PMv-to-M1 pathway, as supported by monkey studies where pharmacological administration of $GABA_A$ agonists in M1 was found to suppress the facilitatory effects of PMv conditioning on M1 corticospinal output (Shimazu et al., 2004). However, we do not rule out the possibility that the SICI reduction may reflect a chain of inhibitory interneurons in M1, with $ccPAS_{PMv\rightarrow M1}$ enhancing the efficacy of PMv synaptic input to inhibitory non-SICI-related interneurons (for example, $GABA_B$-mediated interneurons) via LTP; in turn, these interneurons would suppress the activity of inhibitory $GABA_A$-mediated interneurons involved in SICI, thus ultimately releasing the corticospinal tract from inhibition and contributing to its increased excitability. However, further research investigating multiple inhibitory mechanisms in M1 is needed to validate this possibility. Also, past research has suggested that a reduction in GABAergic activity is a necessary precursor to plastic changes due to motor learning or brain stimulation (Jacobs and Donoghue, 1991; Hess and Donoghue, 1996; Ziemann et al., 2001; Rosenkranz and Rothwell, 2006). While the present findings hint at simple interneuronal mechanisms underlying the SICI reduction, it remains to be investigated whether changes in GABAergic transmission might reflect more systemic and complex interactions critical for the induction of STDP in PMv-to-M1 connections.

While our $ccPAS_{PMv\rightarrow M1}$ protocol might enhance excitatory interneurons in M1, our study suggests those neurons are not the ones involved in ICF (Tian and Izumi, 2022), as we found no modulation of that index.

While the inhibitory and local nature of SICI is well established, the ICF is a more complex measure of intracortical excitation, as it is thought to be influenced by glutamatergic facilitation through NMDA receptors (Ziemann et al., 1998), but also GABAergic inhibition through $GABA_A$ receptors (Tandonnet et al., 2010). Moreover, ICF is thought to result from the recruitment of long-range connections originating from remote areas (Ziemann et al., 1998, 2004), including parietal areas (Koch et al., 2013), and some evidence suggests a possible spinal contribution to ICF (Di Lazzaro et al., 2006). Indeed, prior studies have rarely detected ICF modulation following brain stimulation of M1 (Tian and Izumi, 2022). Thus, further research is needed to directly investigate the aftereffect of $ccPAS_{PMv\rightarrow M1}$ on local excitatory mechanisms in M1, such as short intracortical facilitation (SICF).

Our study presents some limitations. First, our experimental design did not include behavioral tasks, which would have allowed us to draw parallels between physiological changes and functional outcomes; however, because the primary focus of the present work was to highlight the physiological bases of ccPAS, we refrained from including behavioral tasks that could potentially exert further effects on motor physiology due to practice (e.g., Classen et al., 1998). Second, our chosen SICI and ICF protocols were not individualized to obtain comparable inhibition and facilitation effects in all individuals. Moreover, we assessed these indices using separate blocks of ppTMS and spTMS trials, instead of using a randomized intermixed order. While personalizing the protocol could yield more consistent effects (e.g., Murase et al., 2015), we wanted to use stimulation paradigms similar to those employed in other studies that have tested SICI/ICF modulations after plasticity inductions (e.g., Ni and Chen 2008; Russman et al., 2009; Lu et al., 2012; Koch et al., 2013; Amadi et al., 2015), to make better comparative inferences relating to the previous literature. On the other hand, future research could confirm the present results by adopting personalized protocols for SICI and ICF, but also for additional intracortical indices such as long intracortical inhibition (LICI) or short intracortical facilitation (SICF), as these indices could also take part in the observed modulations.

5. Conclusions

Our study confirms prior reports of a gradual enhancement of MEPs during $ccPAS_{PMv\rightarrow M1}$ administration (Fiori et al., 2018; Turrini et al., 2022, 2023) and significantly expands prior knowledge about $ccPAS_{PMv\rightarrow M1}$ aftereffects on PMv-to-M1 connectivity (Buch et al., 2011; Johnen et al., 2015; Chiappini et al., 2020) and motor control (Fiori et al., 2018; Turrini et al., 2023), by providing convergent novel evidence that this protocol also acts locally on M1 – the area of cortico-cortical convergence during $ccPAS_{PMv\rightarrow M1}$. Specifically, we demonstrated that our $ccPAS_{PMv\rightarrow M1}$ protocol relies on excitatory PMv-to-M1 interactions and consistently enhances M1 corticospinal excitability, an effect which could be at least partially mediated by intracortical M1 disinhibition due to a decrease in local GABAergic activity (Stelzer et al., 1994; Castro-Alamancos et al., 1995; Chowdhury and Rasmusson, 2002). These findings highlight the neurophysiological underpinnings of Hebbian plasticity in the human PMv-to-M1 network and could contribute to understanding behavioral changes following induction of STDP. These findings also provide new mechanistic insights into the physiological basis of ccPAS that are relevant for developing novel optimized ccPAS protocols for clinical and experimental settings.

Declaration of Competing Interest

There are no known conflicts of interest associated with this publication and there has been no significant financial support for this work that could have influenced its outcome.

Credit authorship contribution statement

Sonia Turrini: Conceptualization, Data curation, Formal analysis, Software, Methodology, Project administration, Writing – original draft. **Francesca Fiori:** Software, Methodology, Formal analysis, Writing – review & editing. **Emilio Chiappini:** Software, Methodology, Writing – review & editing. **Boris Lucero:** Methodology, Writing – review & editing. **Emiliano Santarnecchi:** Supervision, Writing – review & editing. **Alessio Avenanti:** Conceptualization, Methodology, Project administration, Resources, Supervision, Funding acquisition, Writing – original draft.

Data availability

Data will be made available on request.

Acknowledgments

Project funded under the National Recovery and Resilience Plan (NRRP), Mission 4 Component 2 Investment 1.3 - Call for tender No. 341 of 15/03/2022 of Italian Ministry of University and Research funded by the European Union – NextGenerationEU. Award Number: Project code PE0000006, Concession Decree No. 1553 of 11/10/2022 adopted by the Italian Ministry of University and Research, CUP D93C22000930002, “A multiscale integrated approach to the study of the nervous system in health and disease” (MNESYS). This work was also supported by grants from the Bial Foundation [347/2018], Fondazione del Monte di Bologna e Ravenna [1402bis/2021], and Universidad Católica Del Maule [CDPDS2022] awarded to Alessio Avenanti; grants from ANID, Chilean National Agency for Research and Development [Fondequip EQM210128] awarded to Boris Lucero; and grants from the NIH [R01 AG060981-01] and ADDF-TreatFTD fund [ADDF-FTD GA201902–2017902] awarded to Emiliano Santarnecchi. We thank Arianna Capitanio and Elena Protopapa for their help in data collection.

Supplementary materials

Supplementary material associated with this article can be found, in the online version, at doi:10.1016/j.neuroimage.2023.120027.

References

Albert, N.B., Robertson, E.M., Miall, R.C., 2009. The resting human brain and motor learning. Curr. Biol. 19, 1023–1027.
Amadi, U., Allman, C., Johansen-Berg, H., Stagg, C.J., 2015. The homeostatic interaction between anodal transcranial direct current stimulation and motor learning in humans is related to GABAA activity. Brain Stimul. 8, 898–905.
Avenanti, A., Annela, L., Serino, A., 2012. Suppression of premotor cortex disrupts motor coding of peripersonal space. Neuroimage 6, 281–288.
Avenanti, A., Annella, L., Candidi, M., Urgesi, C., Aglioti, S.M., 2013a. Compensatory plasticity in the action observation network: virtual lesions of STS enhance anticipatory simulation of seen actions. Cereb. Cortex 23, 570–580.
Avenanti, A., Candidi, M., Urgesi, C., 2013b. Vicarious motor activation during action perception: beyond correlational evidence. Front. Hum. Neurosci. 7, 185.
Avenanti, A., Paracampo, R., Annella, L., Tidoni, E., Aglioti, S.M., 2018. Boosting and decreasing action prediction abilities through excitatory and inhibitory tDCS of inferior frontal cortex. Cereb. Cortex 28, 1282–1296.
Bäumer, T., Schippling, S., Kroeger, J., Zittel, S., Koch, G., Thomalla, G., … Muenchau, A., 2009. Inhibitory and facilitatory connectivity from ventral premotor to primary motor cortex in healthy humans at rest–a bifocal TMS study. Clin. Neurophysiol. 120, 1724–1731.
Bencivenga, F., Sulpizio, V., Tullo, M.G., Galati, G., 2021. Assessing the effective connectivity of premotor areas during real vs imagined grasping: a DCM-PEB approach. Neuroimage 230, 117806.
Berardelli, A., Abbruzzese, G., Chen, R., Orth, M., Ridding, M.C., Stinear, C., … Thompson, P.D., 2008. Consensus paper on short-interval intracortical inhibition and other transcranial magnetic stimulation intracortical paradigms in movement disorders. Brain Stimul. 1, 183–191.
Bikson, M., Hanlon, C.A., Woods, A.J., Gillick, B.T., Charvet, L., Lamm, C., … Ekhtiari, H., 2020. Guidelines for TMS/tES clinical services and research through the COVID-19 pandemic. Brain Stimul. 13, 1124–1149.
Borgomaneri, S., Vitale, F., Gazzola, V., Avenanti, A., 2015a. Seeing fearful body language rapidly freezes the observer’s motor cortex. Cortex 65, 232–245.

Borgomaneri, S., Vitale, F., Avenanti, A., 2015b. Early changes in corticospinal excitability when seeing fearful body expressions. Sci. Rep. 5, 14122.
Borgomaneri, S., Vitale, F., Avenanti, A., 2017. Behavioral inhibition system sensitivity enhances motor cortex suppression when watching fearful body expressions. Brain Struct. Funct. 222, 3267–3282.
Boroojerdi, B., Battaglia, F., Muellbacher, W., Cohen, L.G., 2001. Mechanisms influencing stimulus-response properties of the human corticospinal system. Clin. Neurophysiol. 112, 931–937.
Buch, E.R., Johnen, V.M., Nelissen, N., O'Shea, J., Rushworth, M.F., 2011. Noninvasive associative plasticity induction in a corticocortical pathway of the human brain. J. Neurosci. 31, 17669–17679.
Buetefisch, C.M., Revill, K.P., Haut, M.W., Kowalski, G.M., Wischnewski, M., Pifer, M., … Hobbs, G., 2018. Abnormally reduced primary motor cortex output is related to impaired hand function in chronic stroke. J. Neurophysiol. 120, 1680–1694.
Caporale, N., Dan, Y., 2008. Spike timing-dependent plasticity: a Hebbian learning rule. Annu. Rev. Neurosci. 31, 25–46.
Caranzano, L., Stephan, M.A., Herrmann, F.R., Benninger, D.H., 2017. Desynchronization does not contribute to intracortical inhibition and facilitation: a paired-pulse paradigm study combined with TST. J. Neurophysiol. 117, 1052–1056.
Carota, F., Kriegeskorte, N., Nili, H., Pulvermüller, F., 2017. Representational similarity mapping of distributional semantics in left inferior frontal, middle temporal, and motor cortex. Cereb. Cortex 27, 294–309.
Castro-Alamancos, M.A., Donoghue, J.P., Connors, B.W., 1995. Different forms of synaptic plasticity in somatosensory and motor areas of the neocortex. J. Neurosci. 15, 5324–5333.
Cerri, G., Shimazu, H., Maier, M.A., Lemon, R.N., 2003. Facilitation from ventral premotor cortex of primary motor cortex outputs to macaque hand muscles. J. Neurophysiol. 90, 832–842.
Chen, R., Rothwell, J., 2012. Cortical Connectivity. Brain Stimulation For Assessing and Modulating Cortical Connectivity and Function, 1st ed. Springer, Berlin Heidelberg.
Chen, R., 2000. Studies of human motor physiology with transcranial magnetic stimulation. Muscle Nerve 23, S26–S32.
Chen, R., 2004. Interactions between inhibitory and excitatory circuits in the human motor cortex. Exp. Brain Res. 154, 1–10.
Chiappini, E., Silvanto, J., Hibbard, P.B., Avenanti, A., Romei, V., 2018. Strengthening functionally specific neural pathways with transcranial brain stimulation. Curr. Biol. 28, R735–R736.
Chiappini, E., Borgomaneri, S., Marangon, M., Turrini, S., Romei, V., Avenanti, A., 2020. Driving associative plasticity in premotor-motor connections through a novel paired associative stimulation based on long-latency cortico-cortical interactions. Brain Stimul. 13, 1461–1463.
Chiappini, E., Sel, A., Hibbard, P.B., Avenanti, A., Romei, V., 2022. Increasing interhemispheric connectivity between human visual motion areas uncovers asymmetric sensitivity to horizontal motion. Curr. Biol. 32, 4064–4070.
Chowdhury, S.A., Rasmusson, D.D., 2002. Effect of GABAB receptor blockade on receptive fields of raccoon somatosensory cortical neurons during reorganization. Exp. Brain Res. 145, 150–157.
Cirillo, J., Lavender, A.P., Ridding, M.C., Semmler, J.G., 2009. Motor cortex plasticity induced by paired associative stimulation is enhanced in physically active individuals. J. Physiol. 587, 5831–5842.
Civardi, C., Cantello, R., Asselman, P., Rothwell, J.C., 2001. Transcranial magnetic stimulation can be used to test connections to primary motor areas from frontal and medial cortex in humans. Neuroimage 14, 1444–1453.
Classen, J., Liepert, J., Wise, S.P., Hallett, M., Cohen, L.G., 1998. Rapid plasticity of human cortical movement representation induced by practice. J. Neurophysiol. 79, 1117–1123.
Cohen, J., 1992. Statistical power analysis. Curr. Dir. Psychol. Sci. 1, 98–101.
Dafotakis, M., Sparing, R., Eickhoff, S.B., Fink, G.R., Nowak, D.A., 2008. On the role of the ventral premotor cortex and anterior intraparietal area for predictive and reactive scaling of grip force. Brain Res. 1228, 73–80.
Davare, M., Andres, M., Cosnard, G., Thonnard, J.L., Olivier, E., 2006. Dissociating the role of ventral and dorsal premotor cortex in precision grasping. J. Neurosci. 26, 2260–2268.
Davare, M., Lemon, R., Olivier, E., 2008. Selective modulation of interactions between ventral premotor cortex and primary motor cortex during precision grasping in humans. J. Physiol. 586, 2735–2742.
Davare, M., Montague, K., Olivier, E., Rothwell, J.C., Lemon, R.N., 2009. Ventral premotor to primary motor cortical interactions during object-driven grasp in humans. Cortex 45, 1050–1057.
Dayan, E., Cohen, L.G., 2011. Neuroplasticity subserving motor skill learning. Neuron 72, 443–454.
de Beukelaar, T.T., Alaerts, K., Swinnen, S.P., Wenderoth, N., 2016. Motor facilitation during action observation: The role of M1 and PMv in grasp predictions. Cortex 75, 180–192.
Devanne, H., Lavoie, B.A., Capaday, C., 1997. Input-output properties and gain changes in the human corticospinal pathway. Exp. Brain Res. 114, 329–338.
Di Lazzaro, V., Oliviero, A., Profice, P., Pennisi, M.A., Di Giovanni, S., Zito, G., … Rothwell, J.C., 2000. Muscarinic receptor blockade has differential effects on the excitability of intracortical circuits in the human motor cortex. Exp. Brain Res. 135, 455–461.
Di Lazzaro, V., Oliviero, A., Pilato, F., Saturno, E., Dileone, M., Mazzone, P., … Rothwell, J.C., 2004. The physiological basis of transcranial motor cortex stimulation in conscious humans. Clin. Neurophysiol. 115, 255–266.
Di Lazzaro, V., Pilato, F., Oliviero, A., Dileone, M., Saturno, E., Mazzone, P., … Rothwell, J.C., 2006. Origin of facilitation of motor-evoked potentials after paired magnetic stimulation: direct recording of epidural activity in conscious humans. J. Neurophysiol. 96, 1765–1771.
Di Luzio, P., Tarasi, L., Silvanto, J., Avenanti, A., Romei, V., 2022. Human perceptual and metacognitive decision-making rely on distinct brain networks. PLoS Biol. 20 (8), e3001750.
Dum, R.P., Strick, P.L., 1996. Spinal cord terminations of the medial wall motor areas in macaque monkeys. J. Neurosci. 16, 6513–6525.
Fiori, F., Chiappini, E., Soriano, M., Paracampo, R., Romei, V., Borgomaneri, S., Avenanti, A., 2016. Long-latency modulation of motor cortex excitability by ipsilateral posterior inferior frontal gyrus and pre-supplementary motor area. Sci. Rep. 6, 1–11.
Fiori, F., Chiappini, E., Candidi, M., Romei, V., Borgomaneri, S., Avenanti, A., 2017. Long-latency interhemispheric interactions between motor-related areas and the primary motor cortex: a dual site TMS study. Sci. Rep. 7, 1–10.
Fiori, F., Chiappini, E., Avenanti, A., 2018. Enhanced action performance following TMS manipulation of associative plasticity in ventral premotor-motor pathway. Neuroimage 183, 847–858.
Fisher, R.J., Nakamura, Y., Bestmann, S., Rothwell, J.C., Bostock, H., 2002. Two phases of intracortical inhibition revealed by transcranial magnetic threshold tracking. Exp. Brain Res. 143, 240–248.
Fogassi, L., Gallese, V., Buccino, G., Craighero, L., Fadiga, L., Rizzolatti, G., 2001. Cortical mechanism for the visual guidance of hand grasping movements in the monkey: a reversible inactivation study. Brain 124, 571–586.
Fourkas, A.D., Bonavolontà, V., Avenanti, A., Aglioti, S.M., 2008. Kinesthetic imagery and tool-specific modulation of corticospinal representations in expert tennis players. Cereb. Cortex 18, 2382–2390.
Ghosh, S., Porter, R., 1988. Corticocortical synaptic influences on morphologically identified pyramidal neurones in the motor cortex of the monkey. J. Physiol. 400, 617–629.
Hamzei, F., Läppchen, C.H., Glauche, V., Mader, I., Rijntjes, M., Weiller, C., 2012. Functional plasticity induced by mirror training: the mirror as the element connecting both hands to one hemisphere. Neurorehabil. Neural Repair 26, 484–496.
Hebb, D.O., 1949. The Organization of behavior: A Neuropsychological Theory. Wiley.
Hess, G., Donoghue, J., 1996. Long-term potentiation and long-term depression of horizontal connections in rat motor cortex. Acta Neurobiol. Exp. 56, 397–405.
Horn, U., Roschka, S., Eyme, K., Walz, A.D., Platz, T., Lotze, M., 2016. Increased ventral premotor cortex recruitment after arm training in an fMRI study with subacute stroke patients. Behav. Brain Res. 308, 152–159.
Houdayer, E., Degardin, A., Cassim, F., Bocquillon, P., Derambure, P., Devanne, H., 2008. The effects of low-and high-frequency repetitive TMS on the input/output properties of the human corticospinal pathway. Exp. Brain Res. 187, 207–217.
Ilić, T.V., Meintzschel, F., Cleff, U., Ruge, D., Kessler, K.R., Ziemann, U., 2002. Short-interval paired-pulse inhibition and facilitation of human motor cortex: the dimension of stimulus intensity. J. Physiol. 545, 153–167.
Jackson, A., Mavoori, J., Fetz, E.E., 2006. Long-term motor cortex plasticity induced by an electronic neural implant. Nature 444, 56–60.
Jacobs, K.M., Donoghue, J.P., 1991. Reshaping the cortical motor map by unmasking latent intracortical connections. Science 251, 944–947.
Jacquet, P.O., Avenanti, A., 2015. Perturbing the action observation network during perception and categorization of actions' goals and grips: state-dependency and virtual lesion TMS effects. Cereb. Cortex 25, 598–608.
Jeannerod, M., 2001. Neural simulation of action: a unifying mechanism for motor cognition. Neuroimage 14, S103–S109.
Johnen, V.M., Neubert, F.X., Buch, E.R., Verhagen, L., O'Reilly, J.X., Mars, R.B., Rushworth, M.F., 2015. Causal manipulation of functional connectivity in a specific neural pathway during behaviour and at rest. Elife 4, e04585.
Kammer, T., Beck, S., Thielscher, A., Laubis-Herrmann, U., Topka, H., 2001. Motor thresholds in humans: a transcranial magnetic stimulation study comparing different pulse waveforms, current directions and stimulator types. Clin. Neurophysiol. 112, 250–258.
Kemlin, C., Moulton, E., Leder, S., Houot, M., Meunier, S., Rosso, C., Lamy, J.C., 2019. Redundancy among parameters describing the input-output relation of motor evoked potentials in healthy subjects and stroke patients. Front. Neurol. 10, 535.
Koch, G., Del Olmo, M.F., Cheeran, B., Ruge, D., Schippling, S., Caltagirone, C., Rothwell, J.C., 2007. Focal stimulation of the posterior parietal cortex increases the excitability of the ipsilateral motor cortex. J. Neurosci. 27, 6815–6822.
Koch, G., Ponzo, V., Di Lorenzo, F., Caltagirone, C., Veniero, D., 2013. Hebbian and anti-Hebbian spike-timing-dependent plasticity of human cortico-cortical connections. J. Neurosci. 33, 9725–9733.
Koganemaru, S., Mima, T., Nakatsuka, M., Ueki, Y., Fukuyama, H., Domen, K., 2009. Human motor associative plasticity induced by paired bihemispheric stimulation. J. Physiol. (Lond.) 587, 4629–4644.
Kujirai, T., Caramia, M.D., Rothwell, J.C., Day, B.L., Thompson, P.D., Ferbert, A., … Marsden, C.D., 1993. Corticocortical inhibition in human motor cortex. J. Physiol. 471, 501–519.
Kumru, H., Albu, S., Rothwell, J., Leon, D., Flores, C., Opisso, E., … Valls-Sole, J., 2017. Modulation of motor cortex excitability by paired peripheral and transcranial magnetic stimulation. Clin. Neurophysiol. 128, 2043–2047.
Lazari, A., Salvan, P., Cottaar, M., Papp, D., Rushworth, M.F.S., Johansen-Berg, H., 2022. Hebbian activity-dependent plasticity in white matter. Cell Rep. 39, 110951.
Liepert, J., Classen, J., Cohen, L.G., Hallett, M., 1997. Task-dependent changes of intracortical inhibition. Electroencephalogr. Clin. Neurophysiol. 1, 123–124.
Lu, M.K., Tsai, C.H., Ziemann, U., 2012. Cerebellum to motor cortex paired associative stimulation induces bidirectional STDP-like plasticity in human motor cortex. Front. Hum. Neurosci. 6, 260.
Möller, C., Arai, N., Lücke, J., Ziemann, U., 2009. Hysteresis effects on the input–output curve of motor evoked potentials. Clin. Neurophysiol. 120, 1003–1008.
Markram, H., Gerstner, W., Sjöström, P.J., 2011. A history of spike-timing-dependent plasticity. Front. Synaptic Neurosci. 3, 4.

Mayka, M.A., Corcos, D.M., Leurgans, S.E., Vaillancourt, D.E., 2006. Three-dimensional locations and boundaries of motor and premotor cortices as defined by functional brain imaging: a meta-analysis. Neuroimage 31, 1453–1474.
Momi, D., Neri, F., Coiro, G., Smeralda, C., Veniero, D., Sprugnoli, G., … Santarnecchi, E., 2020. Cognitive enhancement via network-targeted cortico-cortical associative brain stimulation. Cereb. Cortex 30, 1516–1527.
Murase, N., Cengiz, B., Rothwell, J.C., 2015. Inter-individual variation in the after-effect of paired associative stimulation can be predicted from short-interval intracortical inhibition with the threshold tracking method. Brain Stimul. 8, 105–113.
Nelles, G., Jentzen, W., Jueptner, M., Müller, S., Diener, H.C., 2001. Arm training induced brain plasticity in stroke studied with serial positron emission tomography. Neuroimage 13, 1146–1154.
Ni, Z., Chen, R., 2008. Short-interval intracortical inhibition: a complex measure. Clin. Neurophysiol. 119, 2175–2176.
Paulus, W., Classen, J., Cohen, L.G., Large, C.H., Di Lazzaro, V., Nitsche, M., … Ziemann, U., 2008. State of the art: pharmacologic effects on cortical excitability measures tested by transcranial magnetic stimulation. Brain Stimul. 1, 151–163.
Peurala, S.H., Müller-Dahlhaus, J.F.M., Arai, N., Ziemann, U., 2008. Interference of short--interval intracortical inhibition (SICI) and short-interval intracortical facilitation (SICF). Clin. Neurophysiol. 119, 2291–2297.
Philip, B.A., Frey, S.H., 2016. Increased functional connectivity between cortical hand areas and praxis network associated with training-related improvements in non-dominant hand precision drawing. Neuropsychologia 87, 157–168.
Pinto, A.D., Chen, R., 2001. Suppression of the motor cortex by magnetic stimulation of the cerebellum. Exp. Brain Res. 140, 505–510.
Prabhu, G., Shimazu, H., Cerri, G., Brochier, T., Spinks, R.L., Maier, M.A., Lemon, R.N., 2009. Modulation of primary motor cortex outputs from ventral premotor cortex during visually guided grasp in the macaque monkey. J. Physiol. 587, 1057–1069.
Ridding, M.C., Rothwell, J.C., 1997. Stimulus/response curves as a method of measuring motor cortical excitability in man. Electroencephalogr. Clin. Neurophysiol. Electromyogr. Motor Control 105, 340–344.
Rizzo, V., Siebner, H.S., Morgante, F., Mastroeni, C., Girlanda, P., Quartarone, A., 2009. Paired associative stimulation of left and right human motor cortex shapes interhemispheric motor inhibition based on a Hebbian mechanism. Cereb. Cortex 19, 907–915.
Rizzo, V., Bove, M., Naro, A., Tacchino, A., Mastroeni, C., Avanzino, L., … Quartarone, A., 2011. Associative cortico-cortical plasticity may affect ipsilateral finger opposition movements. Behav. Brain Res. 216, 433–439.
Rizzolatti, G., Cattaneo, L., Fabbri-Destro, M., Rozzi, S., 2014. Cortical mechanisms underlying the organization of goal-directed actions and mirror neuron-based action understanding. Physiol. Rev. 94, 655–706.
Romei, V., Chiappini, E., Hibbard, P.B., Avenanti, A., 2016a. Empowering reentrant projections from V5 to V1 boosts sensitivity to motion. Curr. Biol. 26, 2155–2160.
Romei, V., Thut, G., Silvanto, J., 2016b. Information-based approaches of noninvasive transcranial brain stimulation. Trends Neurosci. 39, 782–795.
Rosenkranz, K., Rothwell, J.C., 2006. Differences between the effects of three plasticity inducing protocols on the organization of the human motor cortex. Eur. J. Neurosci. 23, 822–829.
Rossi, S., Antal, A., Bestmann, S., Bikson, M., Brewer, C., Brockmöller, J., … Hallett, M., 2021. Safety and recommendations for TMS use in healthy subjects and patient populations, with updates on training, ethical and regulatory issues: expert Guidelines. Clin. Neurophysiol. 132, 269–306.
Rossini, P.M., Barker, A.T., Berardelli, A., Caramia, M.D., Caruso, G., Cracco, R.Q., … Tomberg, C., 1994. Non-invasive electrical and magnetic stimulation of the brain, spinal cord and roots: basic principles and procedures for routine clinical application. Report of an IFCN committee. Electroencephalogr. Clin. Neurophysiol. 91, 79–92.
Rossini, P.M., Burke, D., Chen, R., Cohen, L.G., Daskalakis, Z., Di Iorio, R., … Ziemann, U., 2015. Non-invasive electrical and magnetic stimulation of the brain, spinal cord, roots and peripheral nerves: basic principles and procedures for routine clinical and research application. An updated report from an IFCN Committee. Clin. Neurophysiol. 126, 1071–1107.
Russmann, H., Lamy, J.C., Shamim, E.A., Meunier, S., Hallett, M., 2009. Associative plasticity in intracortical inhibitory circuits in human motor cortex. Clin. Neurophysiol. 120, 1204–1212.
Sanger, T.D., Garg, R.R., Chen, R., 2001. Interactions between two different inhibitory systems in the human motor cortex. J. Physiol. 530, 307.
Santarnecchi, E., Momi, D., Sprugnoli, G., Neri, F., Pascual-Leone, A., Rossi, A., Rossi, S., 2018. Modulation of network-to-network connectivity via spike-timing-dependent noninvasive brain stimulation. Hum. Brain Mapp. 39, 4870–4883.
Schwenkreis, P., Liepert, J., Witscher, K., Fischer, W., Weiller, C., Malin, J.P., Tegenthoff, M., 2000. Riluzole suppresses motor cortex facilitation in correlation to its plasma level. A study using transcranial magnetic stimulation. Exp. Brain Res. 135, 293–299.
Sel, A., Verhagen, L., Angerer, K., David, R., Klein-Flügge, M.C., Rushworth, M.F., 2021. Increasing and decreasing interregional brain coupling increases and decreases oscillatory activity in the human brain. Proc. Natl. Acad. Sci. U. S. A. 118, e2100652118.
Shimazu, H., Maier, M.A., Cerri, G., Kirkwood, P.A., Lemon, R.N., 2004. Macaque ventral premotor cortex exerts powerful facilitation of motor cortex outputs to upper limb motoneurons. J. Neurosci. 24, 1200–1211.
Sinclair, C., Hammond, G.R., 2009. Excitatory and inhibitory processes in primary motor cortex during the foreperiod of a warned reaction time task are unrelated to response expectancy. Exp. Brain Res. 194, 103–113.
Singh, A.M., Neva, J.L., Staines, W.R., 2014. Acute exercise enhances the response to paired associative stimulation-induced plasticity in the primary motor cortex. Exp. Brain Res. 232, 3675–3685.
Stagg, C.J., Bestmann, S., Constantinescu, A.O., Moreno Moreno, L., Allman, C., Mekle, R., … Rothwell, J.C., 2011. Relationship between physiological measures of excitability and levels of glutamate and GABA in the human motor cortex. J. Physiol. 589, 5845–5855.
Stefan, K., Kunesch, E., Cohen, L.G., Benecke, R., Classen, J., 2000. Induction of plasticity in the human motor cortex by paired associative stimulation. Brain 123, 572–584.
Stelzer, A., Shi, H., 1994. Impairment of gabaa receptor function byn-methyl-D-aspartate-mediated calcium influx in isolated ca1 pyramidal cells. Neuroscience 62, 813–828.
Sun, F.T., Miller, L.M., Rao, A.A., D'Esposito, M., 2007. Functional connectivity of cortical networks involved in bimanual motor sequence learning. Cereb. Cortex 17, 1227–1234.
Suppa, A., Quartarone, A., Siebner, H., Chen, R., Di Lazzaro, V., Del Giudice, P., … Classen, J., 2017. The associative brain at work: evidence from paired associative stimulation studies in humans. Clin. Neurophysiol. 128, 2140–2164.
Tandonnet, C., Garry, M.I., Summers, J.J., 2010. Cortical activation during temporal preparation assessed by transcranial magnetic stimulation. Biol. Psychol. 85, 481–486.
Taubert, M., Lohmann, G., Margulies, D.S., Villringer, A., Ragert, P., 2011. Long-term effects of motor training on resting-state networks and underlying brain structure. Neuroimage 57, 1492–1498.
Tian, D., Izumi, S.I., 2022. Transcranial magnetic stimulation and neocortical neurons: the micro-macro connection. Front. Neurosci. 371.
Tidoni, E., Borgomaneri, S., di Pellegrino, G., Avenanti, A., 2013. Action simulation plays a critical role in deceptive action recognition. J. Neurosci. 33, 611–623.
Tokuno, H., Nambu, A., 2000. Organization of nonprimary motor cortical inputs on pyramidal and nonpyramidal tract neurons of primary motor cortex: an electrophysiological study in the macaque monkey. Cereb. Cortex 10, 58–68.
Turrini, S., Fiori, F., Chiappini, E., Santarnecchi, E., Romei, V., Avenanti, A., 2022. Gradual enhancement of corticomotor excitability during cortico-cortical paired associative stimulation. Sci. Rep. 12, 14670.
Turrini, S., Bevacqua, N., Cataneo, A., Chiappini, E., Fiori, F., Candidi, M., Avenanti, A., 2023. Transcranial cortico-cortical paired associative stimulation (ccPAS) over ventral premotor-motor pathways enhances action performance and corticomotor excitability in young adults more than in elderly adults. Front. Aging Neurosci. 15, 1119508.
Ugawa, Y., Uesaka, Y., Terao, Y., Hanajima, R., Kanazawa, I., 1995. Magnetic stimulation over the cerebellum in humans. Ann. Neurol. 37, 703–713.
Valchev, N., Tidoni, E., Hamilton, A.F.C., Gazzola, V., Avenanti, A., 2017. Primary somatosensory cortex necessary for the perception of weight from other people's action: a continuous theta-burst TMS experiment. Neuroimage 152, 195–206.
Veniero, D., Ponzo, V., Koch, G., 2013. Paired associative stimulation enforces the communication between interconnected areas. J. Neurosci. 33, 13773–13783.
Vitale, F., Padrón, I., Avenanti, A., De Vega, M., 2021. Enhancing motor brain activity improves memory for action language: a tDCS study. Cereb. Cortex 31, 1569–1581.
Vitale, F., Monti, I., Padrón, I., Avenanti, A., de Vega, M., 2022. The neural inhibition network is causally involved in the disembodiment effect of linguistic negation. Cortex 147, 72–82.
Wiestler, T., Diedrichsen, J., 2013. Skill learning strengthens cortical representations of motor sequences. Elife 2, e00801.
WMA, 2013. World Medical Association Declaration of Helsinki: ethical principles for medical research involving human subjects. JAMA 310, 2191–2194.
Zanon, M., Borgomaneri, S., Avenanti, A., 2018. Action-related dynamic changes in inferior frontal cortex effective connectivity: a TMS/EEG coregistration study. Cortex 108, 193–209.
Zibman, S., Daniel, E., Alyagon, U., Etkin, A., Zangen, A., 2019. Interhemispheric cortico-cortical paired associative stimulation of the prefrontal cortex jointly modulates frontal asymmetry and emotional reactivity. Brain Stimul. 12, 139–147.
Ziemann, U., Lönnecker, S., Steinhoff, B.J., Paulus, W., 1996a. Effects of antiepileptic drugs on motor cortex excitability in humans: a transcranial magnetic stimulation study. Ann. Neurol. 40, 367–378.
Ziemann, U., Rothwell, J.C., Ridding, M.C., 1996b. Interaction between intracortical inhibition and facilitation in human motor cortex. J. Physiol. 496, 873–881.
Ziemann, U., Corwell, B., Cohen, L.G., 1998. Modulation of plasticity in human motor cortex after forearm ischemic nerve block. J. Neurosci. 18, 1115–1123.
Ziemann, U., Muellbacher, W., Hallett, M., Cohen, L.G., 2001. Modulation of practice-dependent plasticity in human motor cortex. Brain 124, 1171–1181.
Ziemann, U., Iliać, T.V., Pauli, C., Meintzschel, F., Ruge, D., 2004. Learning modifies subsequent induction of long-term potentiation-like and long-term depression-like plasticity in human motor cortex. J. Neurosci. 24, 1666–1672.